Classification and Electrophysiological Analysis of Different Types of Reward and Error in the GPi and ACC



Mehreen Inayat

Kellogg College

University of Oxford

A dissertation submitted for the degree of

Master of Science

Michaelmas 2023

CLASSIFICATION AND ELECTROPHYSIOLOGICAL ANALYSIS OF DIFFERENT TYPES OF REWARD AND ERROR IN THE GPi AND ACC

Mehreen Inayat, Kellogg College

Dissertation submitted for the degree of Master of Science

ABSTRACT

This project aims to examine the dorsal anterior cingulate cortex (dACC) and the globus pallidus internal (GPi) within the context of their cognitive functions from patients that had undergone deep brain stimulation (DBS) surgery. Patients performed the intra-extra dimensional set shifting (IED) task that allowed neural activity from both the dACC and GPi to be recorded while participants got trials correct and incorrect. These trials were categorized beyond these two domains into five different types (expected correct, adjusted correct, guess correct, mistake, and unexpected incorrect) based on their level of surprisingness. Various analytical techniques including event-related spectral perturbation (ERSP), event related potential (ERP), linear regression, Fourier transform, and autoregression were used to examine the neural activity associated with the five conditions. ERSP analysis of the data highlighted that both the dACC and the GPi show differences in frequency power for correct vs incorrect trials and for types of incorrect trials but show no differences when comparing types of correct trials. The ERP analysis alongside linear regression highlighted trends when examining ERP parameters such as maximum ERP amplitude, minimum ERP amplitude, and the amplitude range. A positive correlation was seen as the level of surprise increased for both the maximum ERP amplitude and the ERP range and a negative correlation was seen as the level of surprise increased for the minimum ERP amplitude. A stronger correlation was seen in the dACC compared to the GPi. In addition to looking at the entire trial length of each trial in the IED task, three components of the trials were further examined independently including the decision-making phase, the learning phase, and the peri feedback phase of the trial. This allowed for more focused examination of these nuclei within three different cognitive domains. The Fourier transform and autoregression analyses were used to examine the spectral amplitude and post spectral density respectively of various cognitively significant frequency bands (theta, alpha, beta, gamma, and high gamma). Within the GPi significant differences were found in the gamma/high gamma frequencies during the peri feedback and learning phase of trials when comparing expected correct and unexpected incorrect trials. Within the dACC significant differences were found in the gamma/high gamma frequencies only during the peri feedback phase of the trial. Although greater gamma/high gamma amplitudes were found for the unexpected incorrect condition within the GPi, within the dACC, greater gamma/high gamma amplitudes were found for the expected correct condition. This reversal could indicate that the gamma/high gamma frequency may be one mechanism differentially guiding the learning and memory of correct and incorrect trials within the GPi and dACC. Overall, the results from this project provide evidence in supporting the hypothesis that the dACC and the GPi do serve cognitive functions and are not merely motor nuclei within the brain.

TABLE OF CONTENTS

I. Statement of Authorship.....5

II. Acknowledgements.....5

1.Introduction.....6

1.1 Deep Brain Stimulation.....6

1.2 Reward Learning and Two Distinct Reward Systems.....8

1.3 Introduction of The Anterior Cingulate Cortex: The Early system.....11

1.4 An Introduction to The Dorsal Anterior Cingulate Cortex 12

1.5 Lateralization of the Dorsal Anterior Cingulate: Prediction Errors and Outcome Valence.....15

1.6 Motor Control and Attentional Processing as Output Controls of the ACC……..…17

1.7 Anatomy of the Basal Ganglia.....18

1.8 An Introduction to The Late System of Reward Learning.....20

1.9 Current Study.....21

2. Methods.....24

2.1 Subject Group and Ethics Approval 24

2.2 Surgery 25

2.3 The intra-Extra Dimensional Set Shifting (IED) Task.....25

2.4 Cambridge Electronic Devices (CED) Spike 2 Software.....29

2.5 Data Transfer From Spike2 to MATLAB.....34

2.6 Data Processing with MATLAB & EEGLAB: Loading Data.....35

2.7 Data Preprocessing with MATLAB & EEGLAB.....37

2.8 Data Extraction with EEGLAB: Study Function.....38

2.9 General Theoretical Exploration of Signal Processing Techniques Used in The Project

2.9.1 The Event Related Potential (ERP).....39

2.9.2 Fourier Transform 40

2.9.3 Wavelet Analysis.....41

2.9.4 Autoregression 42

3. Results.....43

3.1 Results Chapter 1: Exploring The Differences Between Correct and Incorrect Trials

3.1.1 Introduction 43

3.1.2 Methods.....44

3.1.2.1 ERSP Images and Statistics 44

3.1.2.2 Linear Regression 47

3.1.3 Results & Discussion 49

3.2 Investigating Differences in Correct and Incorrect Trials With Different Epochs Using Fourier Transform & Autoregression

3.2.1 Introduction 60

3.2.2 Methods 61

3.2.3 Results & Discussion 66

4. Conclusion 74

5. References 77

I. Statement of Authorship

This thesis is all my own work except that the data that was used for analysis was not collected by me. This data has been previously published by Weiss et al. (2018), Keogh et al. (2022), and Gillies et al. (2017). The purpose of this project was to analyze the data in a novel way which I did by sub-classifying trials into different types as well as looking at different cognitive components of the trials.

Secondly, although all the coding scripts used in this thesis are not pre-existing scripts, some of the coding was adapted from parts of existing scripts provided by Martin Gillies MA, BM, BCh, PhD, MRCS, AFHEA, and Habiba Noamany BSc who is conducting her PhD at Harvard University.

II. Acknowledgements

I would like to express my deepest gratitude to my supervisor Dr. Martin Gillies affiliated with the Oxford Functional Neurosurgery and Experimental Neurology Group. He has been there in support of my degree progression in a genuine and caring manner. This degree truly would not have been possible without his supervision, support, guidance, and kindness. I would also like to thank Dr. Alexander Green for giving me the opportunity to join his lab and to be extremely supportive of my degree progression. I have been able to learn a lot of new techniques and skills that I would have never anticipated to have gained without the help of Dr. Gillies and Dr. Green.

I would secondly like to express my love and gratitude for Habiba Noamany who is a PhD student at Harvard University in Boston. I would have never been able to finish this thesis without her. She helped me understand and learn coding in a manner that was essential for me to continue my data analysis. Her numerous hours of zoom meetings have been the reason that I have been able to produce the Fourier transform and autoregression analysis for this project. As part of this thank you, I would like to thank Maryam Dadabhoy who has been a very special friend of mine from our time together at the University of Toronto. Her genuine care and concern for me and the progression of my degree was what led her to connect Habiba and I together.

I would like to thank my friends and family who have been the rock holding me down through this entire degree. This has not been an easy two years and without their support and love I would not have made it to the end of this degree.

1.Introduction

1.1 Deep Brain Stimulation

Throughout time, electrical stimulation has been an important technique used to modulate or treat neurological disorders (Sironi, 2011). The concept of electrical stimulation first began in 46 AD with Scribonius Largo, a physician of the Roman Emperor Claudius. He documented that electric ray fish, which produce electrical discharge, can sooth headaches when placed on the cranial surface. Up until the eighteenth century, these fish served as treatment for seizures, depression, and pain. The idea of electrical stimulation was then further substantiated in the nineteenth century by Giovanni Aldini who performed electrical stimulation on prisoners, discovering that cortical stimulation could cause facial grimaces. Since then, electrical stimulation has become a common tool that is used to both advance our understanding of the brain and its functions, and to provide therapeutic benefits. Newer techniques include transcranial magnetic stimulation, cortical stimulation, and deep brain stimulation (DBS).

For this project, DBS will be discussed in more detail as all patients underwent DBS surgery which involves precise implantation of electrodes in targeted areas of the brain (Sironi, 2011). One of the most common uses of DBS is to help symptoms associated with movement disorders such as Parkinson's and Dystonia. Common targets used for Parkinson's disease include the: subthalamic nucleus (STN), internal globus pallidus (GPi), ventral intermediate nucleus (VIM), and pedunculopontine nucleus (PPN) (Mao et al., 2019). Although the STN and GPi tend to be the most common target areas for DBS and tend to be associated with higher efficacy, there is currently no consensus on an ideal target (Mao et al., 2019). DBS to these target areas can improve Parkinsonian symptoms such as tremors, slowness, stiffness, and walking difficulties (Groiss et al., 2009). DBS of the STN, VIM, and GPi can also aid in treating symptoms of Dystonia (Fan et al., 2021). In terms of surgical practice, target localization occurs based on

stereotactic coordinates and is then personalized using fusion of cranial magnetic resonance imaging (cMRI) and cranial computed tomography (CCT) (Groiss et al., 2009). Intraoperative analyses are also performed to further verify electrode position (Groiss et al., 2009). The electrode itself has four or eight points of contacts that can each be activated separately allowing for minor modifications to be made to the target area (Sironi, 2011; Amon & Alesch, 2017). Prior to DBS surgery being performed, patients must meet predetermined inclusion and exclusion criteria which can vary depending on the underlying condition (Groiss et al., 2009).

Despite the effectiveness and common use of DBS, the exact mechanism of action remains unclear and is debated within the scientific community (McIntyre et al., 2004). There are two general philosophies about the effects of DBS including: 1) when a structure is stimulated, it causes a reversible functional lesion that then inhibits the target area being stimulated or 2) upon stimulation, networks that are part of the target area become activated. Following these philosophies, there are four existing hypotheses about the functional explanation behind DBS including: depolarization blockade, synaptic inhibition, synaptic depression, and stimulation-induced modulation of pathological network activity (McIntyre et al., 2004). Depolarization blockade refers to an alteration in activity of voltage-gated current channels such that neural output near the electrode is blocked upon stimulation. Synaptic inhibition refers to indirect inhibition of neuronal output upon activation of axon terminals that make synaptic connections with neurons near the electrode. Synaptic depression refers to the loss of synaptic transmission of efferent outputs of stimulated neurons due to transmitter depletion. There is evidence to support all these hypotheses but no one hypothesis offers a full explanation of the effects seen after DBS. Current research is analyzing the details of DBS induced changes in neuronal physiology to further explore the details of these mechanisms of actions and how they impact activity on both the single cell and network level.

Even though there is much to learn and discover about the functional mechanisms, the technological advancements, and the application of DBS, it has not only become an efficient therapeutic tool, but has allowed researchers to gather electrophysiological data from the human brain. What makes DBS particularly interesting for this current project is that it provides the means of recording localised voltage-time signals from the targeted areas. Within the context of this project these signals are local field potentials which represent synchronized activity of groups of cells within the nuclei of interest (Lempka & McIntyre, 2013). These recordings are obtained by getting voltage traces from the electrodes that are externalized such that they are connected to an amplifier and digitizer. This allows recordings to be taken on a computer while patients perform various tasks (Weiss et al., 2018). The use of DBS within this context has allowed for substantial advancements in our understanding of the functional anatomy of brain circuits and the relationship between those circuits and various behavioural phenomena (Perlmutter et al., 2006). This technique has set the basis of this current project, as we have gathered and analyzed electrophysiological data from DBS patients that performed a neuropsychological task to explore the connection between neural activity and various behavioural outputs associated with reward-based learning and decision making.

1.2 Reward Learning and Two Distinct Neural Systems

Learning and adapting actions to avoid repeated mistakes while reinforcing rewarding behaviour is essential for human survival (Fouragnan et al., 2015). As an example, if you are out in the forest looking for berries and a swarm of bees (negative outcome) are present, to successfully escape harm, you first need to react by switching your behaviour to move away from the bees, and second learn from the experience to then avoid similar situations in the future. The first theory that described two distinct value systems that first aim to trigger avoidance behaviour and second facilitate learning, was called the reinforcement sensitivity theory (RST). The basis of this theory was that the first value system very

quickly assessed the valence of an outcome (positive or negative), allowing for immediate action, while the second aimed to adjust future behaviour. Secondly, the theory also suggested an interaction between the two systems, such that the first system modulates the second system to update future expectations. In support of this theory, human EEG data has revealed that there is an early valence sensitive system that is driven by an alertness response to negative outcomes and a late system that allows for learning and updated expectations about rewards (Fouragnan et al., 2015).

Much of the background for this current project comes from work done by Fouragnan et al. (2015 & 2017), who utilized electroencephalography (EEG) and magnetic resonance imaging (MRI) technology simultaneously to further investigate these early and late systems. They found that the early system showed greater response activity for negative outcomes compared to positive ones and only responses to endogenous variability for negative outcomes, whereas the late system showed greater response activity for positive outcomes but still correlated with endogenous variability from both positive and negative outcomes. This suggests the idea that the late system can both activate (when there is a positive outcome) and suppress (when there is a negative outcome) relevant brain regions to promote both avoidance and approach learning. Overall, from their first study on this work they were able to conclude that there is a fast (early) system that processes negative outcomes to first initiate a fast alertness and to second, downregulate the response of the late system to facilitate and promote avoidance learning. Altogether this combination allows for a quick immediate change in behaviour and actions associated with the negative outcome while preventing the same behaviour from occurring in the future. On the other hand, a positive outcome seems to predominantly activate brain regions associated with the late system, promoting approach learning.

In a second study, Fouragnan et al. (2017) examined reward learning in more detail by evaluating the reward prediction error (RPE) signal. This signal highlights the discrepancy between outcome expectations and reality across two dimensions including categorical valence and the absolute degree of deviation. The categorical valence refers to whether an outcome is overall better or worse than expected, whereas the degree of deviation refers to how much better or worse the actual outcome is from the expected. Their work examined the encoding of RPEs across its two separate components, RPE valence (positive or negative or signed RPEs) and surprise (the magnitude of the RPE or unsigned RPE) because the authors believed these two components can serve different purposes (Fouragnan et al., 2017; Rouhani et al., 2021). For example, the RPE valence can help determine the direction of learning (positive PRE = approach-based learning, negative PRE = avoidance learning) whereas the surprise dimension can influence the amount of attention and subsequently the degree of learning that actually occurs. When speaking about a negative RPE, this translates into a reward being worse than what was predicted while a positive RPE translates to a reward that was better than what was predicted (Rouhani et al., 2021). The results of this study supported the idea that RPE valence and surprise may serve different purposes as both these outcome dimensions had separate spatial representations despite similar temporal encoding (Fouragnan et al., 2017). The authors were able to conclude that the late system which encodes RPE valence aids in determining the direction of learning (either avoidance or approach) and up regulates the reward system after a positive RPE or down regulates the reward system following a negative RPE. On the other hand, they concluded that the surprise element is responsible for speeding up or slowing down learning processes by modulating attentional resources. Apart from these important findings and conclusions, this paper provides important background for the current study because when evaluating the surprise element, the authors further classified surprise to include a medium element. Usually, surprise is evaluated on a high or low basis, but this paper included a medium level of surprise. The authors were able to, based on neuro electrophysiological data, categorize dimensions of surprise. This is important as

it allows evaluation of surprise outside of its two extreme categories. Using this same idea, our current study aims to categorize types of correct and incorrect trials according to various levels of surprise to check for differences in neural activity between subtypes of correct and incorrect trials.

1.3 Introduction of The Anterior Cingulate Cortex: The Early system

The anterior cingulate cortex (ACC) is one popular brain region that is studied in error driven learning (Cai & Padoda-Schioppa, 2012). With the work of Fouragnan et al. (2015) on an early and late system in reward learning, the ACC is a predominant brain region that is involved in the early system (Cai & Padoda-Schioppa, 2012). Anatomically, the ACC has connections to both the limbic system and the prefrontal cortex making this region critical to both emotional affective and cognitive processes (Stevens et al., 2011). Specifically, activity within the ACC has been related to empathy-related responses, socially driven interactions, and decision making (Lavin et al., 2013). As a core component of the pain network, the ACC is not only active when pain stimuli are received by an individual but also when an individual observes others experiencing pain stimuli. This activation is far more complex as it is modulated by contextual information. When an individual observes another individual receiving pain stimulation and they are prosocial, a greater increase in activity corresponding to the empathy response is observed compared to observing an antisocial individual. This first example speaks to the complex involvement of the ACC in high-level cognitive processes and how it can be modulated by external information. Within the realm of decision making, it was previously thought that the ACC was associated with basic error detection, but it is now believed that the ACC is active in outcome and error monitoring as well as action planning. In general, the current model supports the idea that the ACC is involved in processing the difference between expected and actual outcomes of a given decision and providing outputs to organize behavioural responses. Alongside the evidence that has been mentioned, there are several more studies that strongly support the idea that the ACC is at the centre of high-level contextual

integration and behaviour monitoring. For this reason, the ACC becomes an important area of the brain to further investigate to better understand how the brain monitors performance to regulate behaviour.

1.4 An Introduction to The Dorsal Anterior Cingulate Cortex

There is evidence to suggest that the ACC has several functional subdivisions that distinguish between the cognitive and affective functions of this region (Matthews et al., 2004). While the ventral ACC is seen to be involved in the processing and integration of emotional information, the dorsal anterior cingulate cortex (dACC) is involved in cognitive processes such as response inhibition and error processing. There are three broad functional classifications of the dACC. These classifications include the dACC as a monitor, as a controller, and as an economic structure (Heilbronner & Hayden, 2016). It is important to note that this structure is sometimes referred to as the anterior midcingulate cortex (aMCC) (Touroutoglou et al., 2020).

The dACC as a monitor speaks to the function of the ACC that involves observing the external and internal environment to create a summary report that is then passed to downstream structures (Heilbronner & Hayden, 2016). Most of these monitoring signals occur after decisions are made but, in some cases, this can also occur throughout the decision-making process. Although there is no question that the dACC neurons are involved in the monitoring of error, there is evidence to suggest that errors are one of a broader class of stimuli that the dACC responds to. This idea is supported by the observation that in contexts where errors are likely to occur but do not actually occur, the dACC increases in activity (Brown & Braver, 2005). In addition, even neutral cues that signal the need to change strategy, regardless of error commission, also increase activity in the dACC (Amiez et al., 2005). This data that was inconsistent with the narrow error-monitoring hypothesis of the dACC gave rise to an alternative hypothesis which suggested that the dACC is more broadly involved in conflict monitoring (Heilbronner

& Hayden, 2016). Although this hypothesis is supported by neuroimaging studies, at the single-unit level, evidence appears to be scant and inconsistent (Nakamura et al., 2005; Amiex et al., 2006; Cai & Padoa-Schioppa, 2012; Hayden et al., 2022; Ito et al., 2003; Quilodran et al., 2008). One proposed argument for this discrepancy is that the conflict signals observed could be a by-product of dACC function (Heilbronner & Hayden, 2016). This is consistent with the view that the dACC links context and actions, and that conflict is one factor that impacts the activity of these neurons. When it comes to reward monitoring, the firing rate of single neurons in the dACC are sensitive to the value of an obtained reward, to hypothetical rewards, and rejected rewards (Amiez et al., 2006; Hayden et al., 2009; Blanchard & Hayden, 2014). In addition, some studies have characterized post-outcome dACC responses as a reward prediction error (RPE) which represents the difference between the expected and obtained reward (Kennerley et al., 2011; Matsumoto et al., 2007; Seo & Lee, 2007). The dACC activity is seen to correspond with both signed and unsigned (rectified) RPEs which suggests that the dACC carries a more general control signal that promotes an adjustment or change in strategy (Heilbronner & Hayden, 2016). Furthermore, reward encoding in the dACC is context dependent. In some cases, higher firing rates are observed for smaller rewards and in other cases higher firing rates are observed for larger rewards. All these examples strongly suggest that reward encoding is adaptive within the dACC rather than labeled line.

Monitoring the context is important in being able to then control it through a change of behaviour (Heilbronner & Hayden, 2016). One linkage between the dACC and control is highlighted with its close connections to the motor system (Akkal et al., 2002; Morecraft & Van Hoesen, 1998; Paus, 2001; Shima et al., 1991). While there are some studies that show that neurons in the dACC are sensitive to both reward and movement direction including one that showed radial tuning functions, not all evidence is consistent with this viewpoint (Cai & Padoa-Shioppa, 2012; Isomura et al., 2003; Luk & Wallis, 2009;

Matsumoto et al., 2003; Nakamura et al., 2005; Procyk et al,., 2016; Strait et al., 2016; Williams et al., 2004; Hayden & Platt, 2010; Hoshi et al., 2005; Ito et al., 2003; Kennerley & Wallis, 2009; Matsumoto et al., 2007). Whether the neurons themselves have spatial selectivity may not be clear but what is more readily supported is the idea that spatial selectivity of the dACC is contingent on space being relevant for action selection (Seo & Lee, 2007). A more widely supported idea is that the dACC exhibits control via adjustments (Heilbronner & Hayden, 2016). One study that recorded activity from dACC neurons while monkeys performed an action task, found that the neurons within the dACC responded most strongly when an appropriate action changed to regain a reward (Shima & Tanji, 1998). Consistent with this view, lesion studies have revealed that any lesions to the dACC impair the ability to switch responses and to maintain a new strategy following a switch (Rushworth et al., 2003; Shima & Tanji, 1998; Williams et al., 2004; Cudasama et al., 2013; Kennerly et al., 2006). The last domain by which the dACC controls actions/behaviours is through learning. Learning is different from adjustments and thought to be a more abstract form of control because its consequences are delayed (Heilbronner & Hayden, 2016). Activity in the dACC is closely associated with learning in both primates and rats. In one study, neurons in the dACC were far more active during the active learning phase of a learning task compared to the exploit phase (Procyk et al., 2000).

Lastly, the dACC is thought to be an economic structure, keeping track of the value of offers, the value of non-default options, foraging value, and being involved in action-outcome associations (Heilbronner & Hayden, 2016). When it comes to action-outcome associations, one possible function of the dACC can be to serve as an action-outcome predictor. This means that the dACC signals the outcomes associated with specific actions. This is in line with a more unified function of the dACC which states that neurons in the dACC signals predictions which subsequently encodes expectations for likely outcomes of certain actions/decisions. Once feedback has been received the neurons signal valence (either positive or

negative) and respond to the valence via a prediction error signal. This information then gets used to update the previous predictions and guide/optimize future behaviour (Weiss et al., 2018).

Much of the research discussed highlights how the dACC ultimately is important for motor control. The mentioned research describes some of the ways by which this area influences motor responses. However, it does have direct roles in motor movement as well. Specifically, it is known to be important in preparing and implementing a motor action (readiness) (Touroutoglou et al., 2020). Evidence of this is seen in many studies that have found functional activity in this region in response to movement selection, both functional and anatomical connections between this region and other motor areas like the premotor area, consistent activation of this region in response to motor response suppression and initiation, and how stimulation of this area results in complex and simple movements (Touroutoglou et al., 2020;Cunnington et al.,2002; Hoffstaedter et al., 2013; Weiss et al., 2018; Asemi et al., 2015). These studies have led many researchers to believe that the dACC/aMCC is a motor nucleus. However more recent studies are interested in examining this structure within the cognitive domain. An important aim of this project is to determine whether there is evidence to suggest that the dACC has a cognitive functional significance outside of motor control.

1.5 Lateralization of the Dorsal Anterior Cingulate: Prediction Errors and Outcome Valence

Two important studies have further investigated the role of the dACC in hopes of identifying lateralized functions (Weiss et al., 2018; Keogh et al., 2022). Both studies investigated the function of the dACC by analyzing local field potentials (LFPs) of patients who had undergone deep brain stimulation surgery as they performed the intra-extra dimensional set shifting (IED) task. Weiss et al. (2018) first analyzed the reaction time of the participants and found that the reaction times of the second consecutive correct (i.e., when participants had two correct trials in a row) trials were significantly faster than the

second consecutive incorrect trials (i.e., when participants had two incorrect trials in a row). Second, when they averaged the LFPs from both the right and left dACC at the time of stimulus presentation across all trials, they found that feedback was associated with an event-related potential (ERP) that began 50ms after the start of the feedback in the left hemisphere with a higher peak magnitude than in the right hemisphere. When analyzing the post-feedback ERP, they found that there were two distinct temporal components peaking at 200ms (early) and 350ms (late) corresponding to a 6.6Hz or one theta frequency oscillation (3-8Hz) period apart. Both the early and late components are seen to be driven predominantly by negative outcomes. The most marked finding from Weiss et al. (2018) was that the dACC signals when the outcomes of decisions are unexpectedly incorrect. They also provide strong evidence to support the idea that the dACC signals both prediction errors and valence.

A Second study by Keogh et al. (2022) further analyzed the laterality of the dACC and firstly found that a reduction in variance across all channels occurs around -200ms as well as a phase reset which altogether indicates a coherence in the dACC network immediately prior to feedback. They then found a double peaked response after feedback which corresponds to the early and late response. When analyzing the peri-feedback epoch, they found that activity in the left dACC varies from 500ms before feedback to 200ms before feedback but synchronizes with the right dACC 200ms before feedback. These different responses in the right and left dACC further support the idea that there is lateralization of function in the dACC. When analyzing individual sources for the left dACC, the first source showed a peak in the -500ms to 0ms interval and a trough at 250 ms post feedback suggesting that this may be related to the movement of the right hand to the immediate feedback response. The second source showed a double-peaked structure post-feedback, likely relating to the feedback response. The third source showed a response in the +200 to +500 ms post feedback interval which again suggests that this related to the feedback response. when analyzing the sources on the right side, the first source appeared to be related to

the feedback response with a sharp peak and damped double peak structure. The second source showed a distinction between the response at 500 ms and at 200ms pre feedback whereas the third source showed a prolonged trough during the 500ms prediction window. When analyzing communication between the right and left dACC, it was found that there was bidirectional communication between both regions in the -200ms pre-feedback period in alpha and gamma bands. However, the left dACC activity preceded the right by 20ms and it was not altered by outcome valence. Communication also seems to flow left to right post feedback, but in this case the dynamics of information flow was altered by feedback valence. Specifically, for incorrect trials there was greater left to right information flow. These results are important as they first show that information flows asymmetrically in the dACC since it primarily goes from left to right after feedback which is altered by the outcome valence and further modified by learning. These studies both further advance our understanding of the human dACC by anatomically distinguishing its various functions and lays the foundation for the current project.

1.6 Motor Control and Attentional Processing as Output Controls of the ACC

The function of the ACC in relation to error processing has been dissected in detail above, but an important goal of the early system is to be able to allow for a quick change in actions, and or behaviour to avoid a negative outcome. As mentioned above, the ACC is an important structure in the early system and therefore this section will aim to summarize how the ACC contributes to motor function. Anatomically, the ACC has extensive connections with the motor cortex and the spinal cord (Paus, 2001). It has been noted that upon stimulation of the ACC, there is a production of body movement and vocalizations that occur while lesions of the ACC lead to deficits in spontaneous initiation of movement and speech (Womelsdorf et al., 2010). In addition, lesions to the ACC have shown to interfere with willed control of action which is the ability to overcome inertia when initiating actions and fighting competing innate tendencies (Paus, 2001). This very strongly suggests that the ACC can assist in the immediate change of

actions needed in relation to a negative outcome. In addition, the early system is important for modulating future behaviour by enhancing learning. One way this occurs is through modulation of attentional resources. Therefore, the ACC as an important component of the early system needs to play a role in attention and arousal. This is supported by anatomical features such that, there are several afferents to the ACC from thalamic nuclei and the brainstem (areas that are important for alertness and arousal). It has also been seen that activation of the ACC covaries with activation of midline thalamic nuclei. Overall, these findings support the idea that the ACC is an important structure for the early system when looking at error-based learning.

1.7 Anatomy of the Basal Ganglia

To begin with, the basal ganglia (BG) refer to a collection of nuclei located deep in the brain, specifically consisting of the caudate nucleus, putamen (together known as the dorsal striatum), globus pallidus (GP), substantia nigra, and the subthalamic nucleus (STN) (Lanciegoe et al., 2012). From studies conducted in the past, it was widely accepted that the BG plays a very important role in motor control as lesions of the BG would lead to parkinsonian signs, dystonia, and hemiballismus (Lanciego et al., 2012). The broad categorization of these nuclei includes input nuclei, output nuclei, and intrinsic nuclei. Input nuclei such as the caudate and putamen, receive information from other structures in the thalamus, cortex, and nigral regions. The output nuclei of the BG are the globus pallidus internal (GPi) and the substantia nigra pars reticulata (SNr) which send information to the thalamus which then sends projections to the cortex. The other nuclei are considered intrinsic nuclei which relay information between the input and output nuclei. In the BG circuitry, the main transmitter of function is dopamine. This is why dopamine dysfunction is associated with parkinsonian syndrome, dystonia, chorea, and tics. In simple terms, the overall circuit has both a direct and indirect pathway that serve opposing functions. The direct pathway comes from the striatum which sends GABAergic inputs to the output nuclei of the basal ganglia (GPi

and SNr) thus inhibiting these regions. Activation of the indirect pathway ultimately results in activation of the output nuclei (GPi and SNr). Functionally activation of the direct pathway facilitates movement and activation of the indirect pathway results in inhibition of motor activity. The role of dopamine is important in this pathway as the neurons that cause activation of the direct and indirect pathways are modulated by dopamine via D1 and D2 dopamine receptors such that, dopamine depletion causes a reduction in the activity of the direct pathway while simultaneously increasing the activity of the indirect pathway. Overall, this causes an increase in the activity of the GPi and SNr, causing movement inhibition. This pathway is summarized in figure 1.

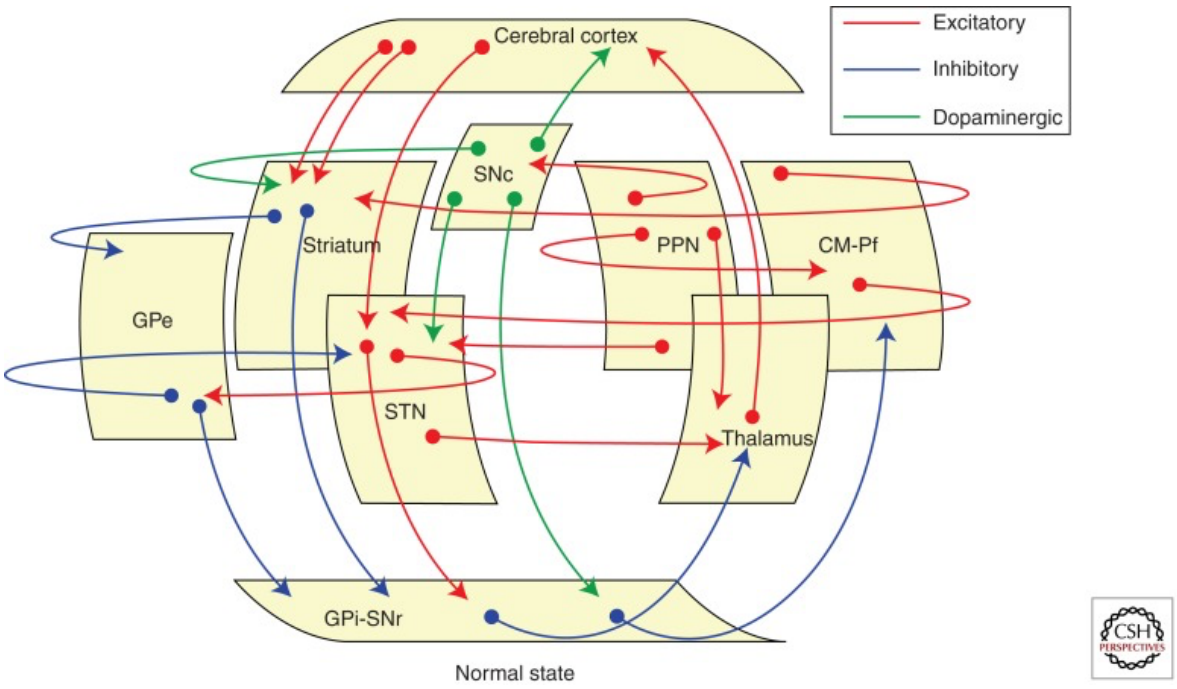


Figure 1. The Basal Ganglia Circuit
This figure is from a paper by Lanciego et al. (2012). It aims to show the circuitry of the basal ganglia, its various inputs, and outputs, as well as the nature of the connections (i.e., whether they are excitatory or inhibitory).

1.8 An Introduction to The Late System of Reward Learning

As mentioned by Fouragnan et al. (2015) there is a late system that is concerned with adapting future actions and behaviour guiding either avoidance or approach learning. To further examine this late system, this project will consider the BG as the brain network of interest. Although the basal ganglia has not been well studied in this context, since there are major dopamine afferents that project to this structure, and it is an important motor output structure, we believe that the basal ganglia can serve as an important structure for this late system of reward processing. There is a lot of evidence that shows an increase in striatal dopamine for a positive prediction error (when a better than expected) or an unexpected reward is received while decreasing when there is a negative prediction error (when a reward is worse than expected) or surprisingly omitted (Doll & Frank, 2009). We also see that there is synaptic modification that occurs within the corticostriatal pathway (Doll & Frank, 2009; Mulcahy et al., 2020; Kim et al., 2017). The general theory surrounding how reward learning is mediated in the basal ganglia depends on three important things. The first being the valence of the reward prediction error, the second being long term potentiation, and the third being long term depression (Kim et al., 2017). When the outcome is better than expected (positive RPE) firing rate of substantia nigra neurons increases and so projections to D1 receptor containing medium spiny neurons become potentiated (i.e., activation of the direct pathway and motor facilitation) and projections to D2 medium spiny neurons become depressed (i.e., less activation of the indirect pathway and motor facilitation). On subsequent trials, the direct and indirect pathways are activated more and less respectively, promoting the same action selection to occur (i.e., a form of approach learning). If a reward is worse than expected (negative RPE), the dopamine that is released varies in magnitude and causes D1 based projections to be depressed while potentiating D2 projections. This reduces activation of the direct pathway thus, inhibiting movement, and causes greater activation of the indirect pathway, also inhibiting movement (i.e., a form of avoidance learning). For these reasons, we are interested in further studying the basal ganglia and how it responds to different types of

rewards within the human brain as work on this remains novel. Having data from human patients that have undergone DBS makes it possible to determine and examine electrophysiological differences in reward processing within the basal ganglia.

1.9 Current Study

The basis for this study builds off the work done by Fouragnan et al. (2015 & 2017) which highlights the idea of two distinct systems involved in reward-based learning and classifies behavioural psychology measures from an electrophysiological perspective. As described in detail, the early system comes into play when there is a negative outcome associated with a particular behaviour/action. This system allows a quick change in behaviour to avoid immediate harm and down regulates the late system. The late system in turn is responsible for the long-term learning process that either enables a behaviour/action to persist in the presence of a positive outcome (approach learning) or results in avoidance learning in the presence of a negative outcome to prevent similar behaviours/actions from occurring in the future.

This study will aim to utilize patients' performance on the IED task. This task is a modified version of the Wisconsin card-sorting cognitive test (Weiss et al., 2018). The IED task measures attentional set shifting, assessing both cognitive flexibility and executive function. At the basic level this task requires the ability to switch between arbitrary internal rules. Due to the variables involved in this task, it is used to identify abnormalities in executive function in various disorders. Processes such as discriminative learning, reversal learning, and the switching of attention can be selectively measured with this task. The task involves choosing between a pair of stimuli, where only one is the correct stimuli and the other is the incorrect stimuli according to a rule that is unknown to the subject. The correctness or

incorrectness of a choice is indicated through auditory feedback following stimulus selection. The objective is for the participant to be able to learn the rule at play through feedback which is indicated by several (six) correct trials in a row. After a rule is learnt successfully and six correct trials have been reached, the rule changes unexpectedly and the participant must adjust their responses and learn the new rule. Since this task contains different dimensions: 1) a rule unknown to the participant must be learnt through guessing, 2) once a rule is learnt it must continue to be executed, and 3) a rule must be unlearnt and a new rule learnt in its place based on provided feedback, it allows for different types of correct and incorrect trials to take place. The analytical aim of this current project is to subclassify correct and incorrect trials to further evaluate differences in electrophysiological activity within the BG and the ACC by examining event-related potentials, and changes in the various biologically relevant frequency bands (theta, alpha, beta, gamma, and high gamma).

General classification of the incorrect trials can correspond to two types of errors. The first error can be classified as a simple mistake which would occur when participants have had some consecutive correct trials and have then had an incorrect trial followed by several correct trials. In this case, the rule would have been learnt by the participant, but they had just made a motor mistake. This would be identified in the raw data as consistent 3-4 correct trials (ensuring that the rule has been learnt and it's not by chance), followed by one incorrect trial, followed by six subsequent correct trials. This type of error could also lead to the generation of a negative RPE as an expected reward (getting a trial correct) has been omitted. A second type of error would be classified as an unexpected error which would occur when the stimulus remains the same, but there has been a sudden change in the rule of the task. This can be identified when participants will have scored six correct trials in a row and will subsequently have an incorrect trial, as the rule changes after six correct trials but the stimulus remains the same. This would also result in a much stronger negative RPE as patients are fully expecting a reward that has now been

omitted. When it comes to classification of correct trials, the first one will include a surprise correct (when a patient does not know the rule and must guess to learn). The second type of correct will include an adjusted correct which will be identified by a correct trial that subsequently follows a previous incorrect trial. This may result in a positive RPE as previously the participants had gotten an incorrect trial and have now successfully received a reward. The last type of correct will be called an expected correct and will include the 6th correct trial as the rule is successfully learned by this point. This would represent a PRE of zero as participants receive the expected reward. These classifications are subjective, further adding to the novelty of this project as this has not been attempted before. This project can also provide a means by which correct and incorrect trials can more consistently be categorized for future studies. Based on these different classifications and how they impact the speed at which participants need to learn to adjust their behaviour as well as the type of learning they need to engage in provides the rationale for why we believe that the basal ganglia and the ACC may show distinct electrophysiological differences between the different classifications.

The first goal of this project deals with analyzing performance for the entire duration of the IED task through event-related spectral perturbations (ERSPs) which show visual changes in amplitude of various frequencies present. This gives a means of evaluating frequency differences between the various types of correct and incorrect trials. The second goal of this project aims to examine properties of the event related potential by performing a linear regression analysis on the maximum, minimum and amplitude range. This analysis relies on the Rescorla-Wagner model of learning. Details of how this model was applied can be found in the methods section of the first results chapter. The last goal of this project is to examine various epochs that focus on different components of trials including decision making, learning, and peri-feedback across various cognitively functional frequencies.

With this analytical plan, both the late system (basal ganglia data) and the early system (ACC data) will be examined with respect to how these areas of the brain respond to various types of correct and incorrect trials. A few key aspects of this project make it novel, the first being that it is an evaluation of the GPi. Much of the literature that exists is surrounding the striatum which is the input region of the basal ganglia. Since the GPi is predominantly the motor output of the basal ganglia it has not been studied in detail in the context of reward learning. The second aspect of this project that makes it novel is the sub classifications of correct and incorrect trials beyond these two major classifications. These investigations together lay the foundation for further examining the GPi and the dACC, both predominantly known for their role in motor control, within the realm of cognition and decision making. The overarching question of this thesis is to determine whether the GPi and the dACC serve cognitive significance within reward and error learning outside their usual motor implications.

2. Methods

2.1 Subject Group and Ethics Approval

For this project, previously collected data from Weiss et al. (2018), Gillies et al. (2017), and Keogh et al. (2022) was used. Data collection did not occur, but rather existing data from these publications were analyzed in novel ways. The details concerning subjects, ethics approval, surgical procedures, and the IED task were taken from these papers. Three types of patient data were analyzed. The first group of patients have idiopathic Parkinson's disease and consist of three people ages 44, 55, and 66. Within these patients there were two different conditions that were looked at. In the first condition, the patients were tested on the IED task without being given dopaminergic medications termed the 'off' medication condition. In the second condition, the same patients were then tested again once they had been given dopaminergic medications. The second group of patients consists of five people (three male and two female) who have focal Dystonia ages 21, 53, 59, 65 and 66 at the time of testing. The

dystonia patients were not on any anti-dystonic medication at the time of testing. All patients had given informed written consent, and the study was approved by Oxfordshire Research Ethics Committee A (Ref 08/H0604/58 & 11/SC/0229). The third group of patients consisted of four chronic pain patients (two male and two females) with an average age of 42. Data obtained from these patients was also carried out with the approval of Oxfordshire Research Ethics Committee A (Ref 1/SC/0229). All three patient groups consisted of right-hand dominant patients and every patient gave informed consent in accordance with the Declaration of Helsinki.

2.2 Surgery

The Parkinson's and Dystonic patients all underwent bilateral globus pallidus deep brain stimulation surgery using a standard technique taken from Yianni et al. (2011). Much of the detail surrounding the surgical procedure can be found in a paper published by Gillies et al. (2017) examining the cognitive role of the GPi. Medtronic 3387 ® DBS leads were placed in bilateral posteroventral GPi. The electrodes had four circumferential 1.5mm contact points separated by 1.5mm. To check the position of the electrodes, a CT scan was performed before recovery from anesthesia which was also verified by Image Fusion with the preoperative MRI. Internalization of the DBS leads, and implantation of the internal pulse generator took place a week later. For the dACC patients all surgical details can be found in Weiss et al. (2018). As a summary, patients underwent bilateral dACC DBS surgery, targeted using preoperative MRI scans. Targets were 20mm posterior to the frontal horns and 8-10mm lateral to the midline to target the dACC. The same electrode dimensions were used for these patients as well. Internalization also happened in a separate session a week after the electrodes were implanted.

2.3 The intra-Extra Dimensional Set Shifting (IED) Task

As mentioned in the introduction the subjects performed the IED task (Cantab ®). There are nine discrimination rules that participants must learn by choosing between a pair of stimuli. Rules of the task are explained to the participants before they begin, informing them to pick one of the two on-screen visual objects (Weiss et al., 2018). Subjects are informed that one of objects present is correct and the other is incorrect, and that the outcome of their performance is delivered by auditory feedback which comprises a tone (pure tone for correct, low frequency modulated pure tone for incorrect). In addition, simultaneous presentation of a coloured box occurs around the edge of the screen (green for correct and red for incorrect) with the word correct or incorrect for 0.5 seconds. The subsequent trial starts 2.7 seconds after the start of the previous trials auditory feedback. They are also informed that the rule will change over the course of the test but that these rule changes are infrequent and happen once the previous rule has been learnt. Subjects are unaware of how many correct trials will result in a rule change or how many times the rule will change. Subjects used their dominant (right hand) for object selection. A rule is defined as learnt when there are six correct trials in a row. At the beginning of the test, the stimuli represent an internal dimension where each of the two visual objects are composed of a single solid abstract shape. As the task progresses, the visual objects gain an external dimension by gaining an additional abstract element in the form of white lines. These lines act as a distraction since the rule itself is only based on the solid shapes. Once rule six is in play, an intradimensional shift occurs as the solid shapes change to two new visual objects composed of new solid shapes and white lines. These white lines govern correct object choice during rule eight which is the extradimensional shift phase of the task. The subject passes the test if all nine rules are learnt in sequence. The subject fails if six correct trials are not achieved in sequence out of 50 trials of a single rule. Rules only change when patients get six consecutive correct trials in a row. Visual details of the sets of rules present and the time components of the task can be found in figure 2 and 3.

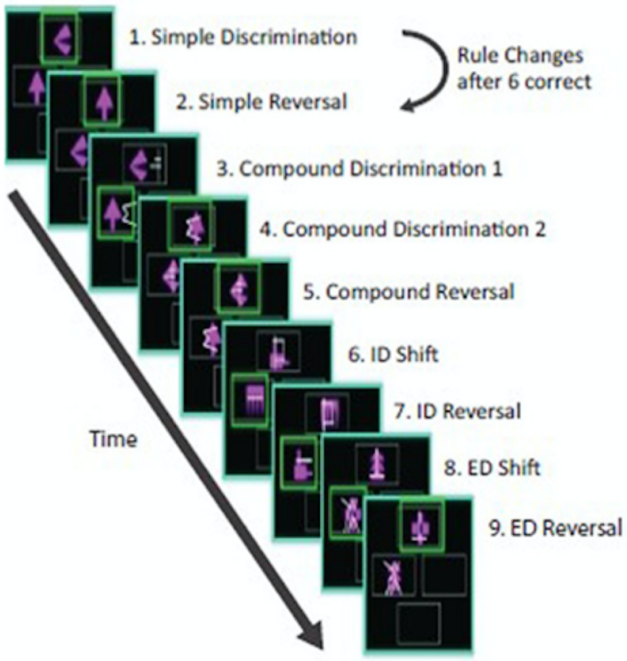


Figure 2. The Stages of the IED Task

This is a visual of the IED task from Weiss et al. (2018) showing its nine different stages. Participants always choose between one of two images, consistent with an unknown rule. Patients must learn the rule by picking an object. Simple discrimination refers to picking between two solid objects. Simple reversal refers to the same visual stimuli being presented but the rule switching so that the previously incorrect object is now the correct object. Compound discrimination 1 and 2 refers to a solid object as well as a 2-D line being shown simultaneously, and the participants must guess whether the rule depends on the white lines or the solid object. At this stage, the solid object still guides the correct choice. Compound reversal refers to the same reversal seen in simple reversal except that both a solid object and a line are present (more complex visual stimuli). Intra-dimensional (ID) shift refers to the solid objects changing to new objects while the lines remain the same. ID reversal is the same as simple reversal just with the new solid objects this time. The extra-dimensional (ED) shift refers to the lines guiding the correct choice rather than the solid objects. Up until this point, it was always the solid object that governed the correct choice. The ED reversal refers to the second line that was previously incorrect now becoming the right choice.

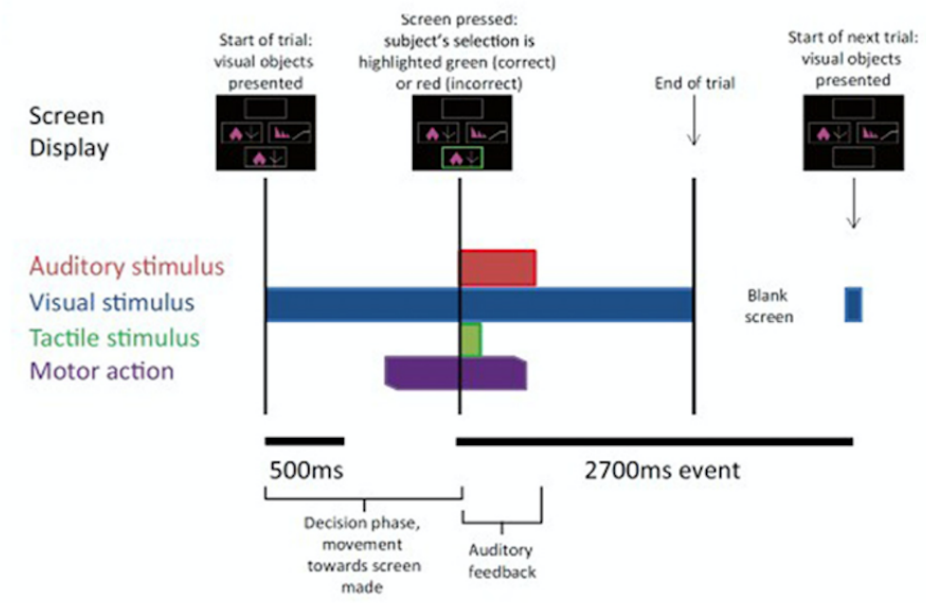


Figure 3. The Time Components of the IED task

This image from Weiss et al., (2018) describes the temporal features of the task. The task is composed of four different components. There is an auditory stimulus (orange) which is presented after the participant has made a choice between two objects and it will indicate the feedback for the trial since there are different tones presented with correct and incorrect trials. The visual stimuli component (blue) refers to the objects being presented on the screen or the presentation of the screen. There are always only ever two objects presented at a time. Tactile stimulus (green) refers to the participant touching the screen to make a decision of which object is correct. Lastly the motor action (purple) refers to the process where the participant reaches out from rest toward the screen and back to rest. Each trial is between 500ms to 2700ms in length. 500ms is the time range at which the visual stimuli are shown, a decision is made, and a movement towards the screen is made. After the 500ms mark is when the auditory stimulus is presented, movement back to rest is made and the participant visually sees whether their answer was correct or incorrect.

2.4 Cambridge Electronic Devices (CED) Spike 2 Software

Data from the IED task was acquired using Spike2. Spike2 is a type of data acquisition and analysis software that deals with continuous multi-channel data (Cambridge Electronic Design Limited, 1988). This software is commonly used in the field of electrophysiology, neurophysiology, cardiovascular and respiratory studies, sports science, and pharmacology. Spike2 allows people to extract data into various other data formats such as spreadsheets, text, binary, and MATLAB files, so that other platforms can be used for further analysis. For these reasons, the initial data acquired used Spike2. Previously acquired data files were further processed on Spike2 by creating event marker cursors. These cursors highlighted time points of interest for six recording channels, marking different types of correct and incorrect trials. Since the task had auditory feedback to inform the participant of a correct and incorrect choice, it was possible to place these cursors at the relevant time points (when the participants received the feedback). It was also possible to sub classify different types of correct and incorrect trials due to the nature of the task. It is important to note that although we did attempt to sub classify different correct and incorrect trials, this was a subjective process and only classifications that could be consistently observed were chosen for analysis. There were three types of correct trials that were chosen:

1) Expected Correct: This was the 6th consecutive correct trial before the task moved to the next rule/shift. It was termed expected correct because when the participant gets six correct trials in a row it is defined as them having learnt the current rule in play and is the point at which the task moves to the next stage. In this case, they are expecting to get the answer correct (Figure 4).



Figure 4. Expected Correct on Spike2
This is an example of an audio channel on Spike2. This shows what a correct choice looks like on the audio channel, and it shows six correct trials in a row indicating that the participant has learnt the given rule in play. The 6th correct marked in black would represent an expected correct because this is the point where a rule is taken as successfully learnt and the task switches to the next rule.

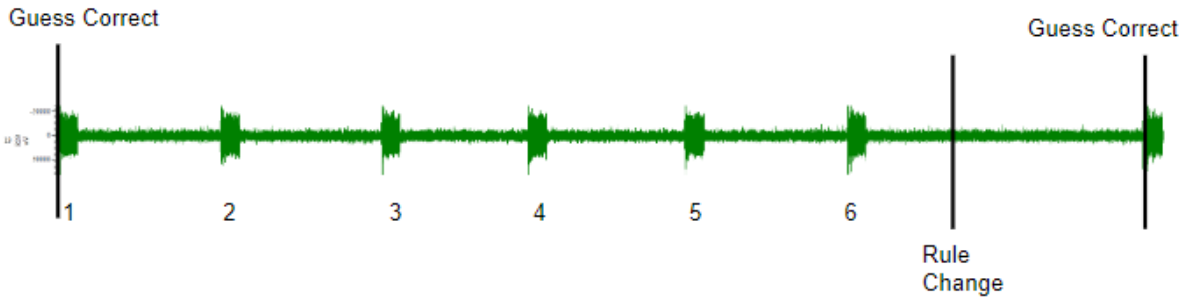
2) Adjusted Correct: This was a correct trial that was followed by a previous incorrect trial followed by consecutive correct trials. The aim of this type of correct trial is to identify a correct trial that the participant used to adjust their behaviour for corresponding trials. It represents participants learning from their mistakes and correcting their decision for future trials (Figure 5).



Figure 5. Adjusted Correct on Spike2
This is an audio channel on Spike2 showing what an adjusted correct trial would look like. In this case participants will have gotten a correct trial following a previous incorrect trial, followed by several correct trials (4-6 correct trials). This shows an adjustment in behaviour to indicate that the participant has learnt from their mistake and adjusted the behavioural output to get the subsequent trials correct.

3) Guess Correct: This is a type of correct when the participant does not know what the rule in play is. It can be observed as the very first trial of the task and can subsequently be found at points of the task where the visual stimulus has changed, and the participant must make a choice to figure out what the new rule in play is. This can be found at compound discrimination 1, compound discrimination 2, ID shift, and ED shift trials. A guess correct can also be classified as a trial where participants appear to be getting correct trials and the rule has not been learnt. An example of this is when there are several incorrect trials and then one or two correct trials followed by more incorrect trials. This would also be indicative of the participant needing to learn the rule and engaging in guessing to figure out which answer is correct (Figure 6).

A



B



Figure 6. Guess Correct Trial on spike2.
A-B) This is an example of an audio channel in Spike2 that show guess corrects. This can occur in three instances, the first is at the very beginning of the task when the participant first starts the task. The very first trial is a guess because the participant does not know what rule is in play and they do not have

previous information to make a decision from (**A**). The second type is when compound discrimination, an ID shift, and or an ED shift occurs. In all these cases the visual stimuli on the screen changes and so the participant must re-determine the rule at play. This is usually visually seen as a correct trial after six consecutive trials (**A**). The last type of guess correct is when the participant has a correct trial that is both followed by an incorrect trial and a previous incorrect trial. This is indicative that the participant has not yet learnt the rule and is guessing to figure it out (**B**).

These different types of corrects aim to highlight different levels of cognitive processing that may need to take place as they are associated with different levels of surprise and require a different level of behavioural adjustment. For example, an expected correct may not require any quick adjustments in behaviour as the participant is fully expecting that their behaviour/action is the correct choice so this would require less attention, and no behavioural adjustment. For something like an adjusted correct, higher attentional resources and quicker cognitive processing may be necessary so the participant can learn from the trial and apply it to future trials. In a guess correct, participants may also need to pay extra attention as they are in the process of learning. In addition, errors or incorrect trials were classified into two types:

1) Mistake: a mistake was classified as an incorrect trial following several correct trials, followed by several correct trials (usually six consecutive trials). This type of pattern in the audio channel can be indicative of a motor mistake made by the participant as they had gotten many trials correct consecutively, and after the incorrect trial proceeded to get more consecutive trials correct (Figure 7).

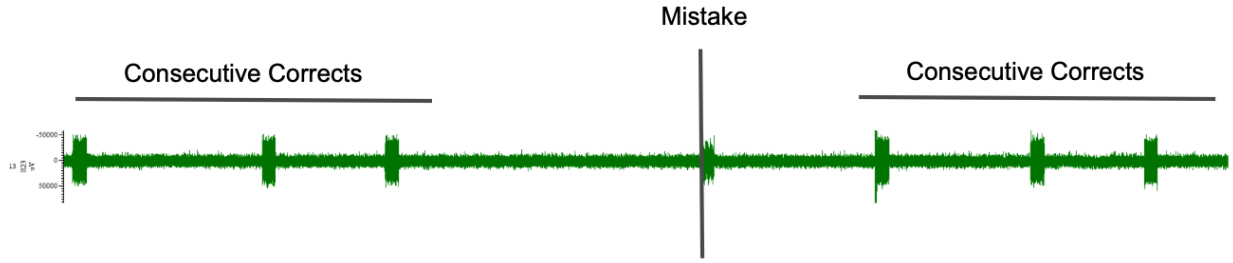


Figure 7. Mistake Trial on Spike2
This is an audio channel example of a marked mistake incorrect trial. This shows three consecutive correct trials indicating that the participant had most likely learnt the rule and made a mistake because there are also more consecutive correct trials after the incorrect trial.

2) Unexpected Incorrect: This type of incorrect deals with the reversal learning stages of the task. During the reversal learning phase of the task, the visual stimulus from the previous rule stays the same but the underlying rule unexpectedly changes. Patients think that the old rule is still in play and end up getting the trial incorrect but are not expecting this as nothing indicates that the rule has now changed. They then must learn the new rule at play. This incorrect is classified as the incorrect trial that subsequently follows six consecutive correct trials and happens specifically at rule change 2, 5, 7, and 9. This can be reliably identified because we know that the rule changes after every 6th correct trial (Figure 8). The total number of trials present in each condition are summarized in Table 1.

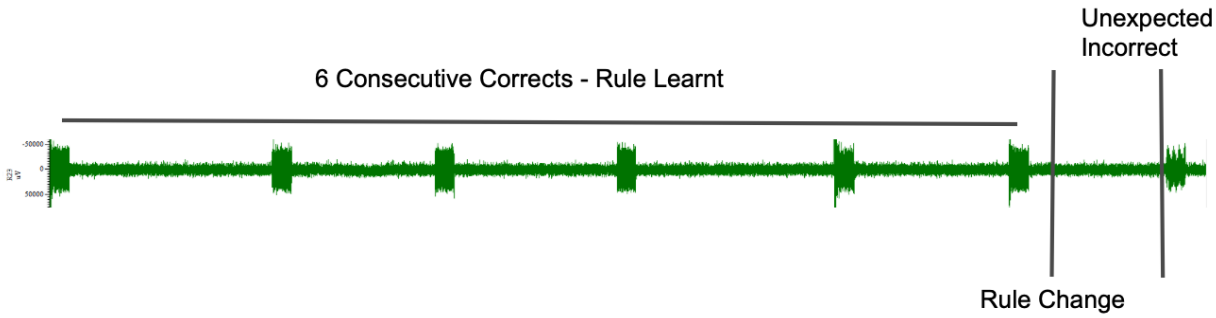


Figure 8. Unexpected Incorrect Trial on Spike2
This is an example of an audio channel for an unexpected incorrect trial. This will occur after 6 consecutive correct trials and is most reliably found at stages 2, 5, 7, and 9 because changes at these phases of the task are specific to reversal learning where the visual stimuli stay the same, but the underlying rule has changed without the patient knowing.

Table 1. The number of trials present in each type of correct and incorrect trial for both the GPi (dystonic patients) and the dACC (chronic pain patients).

Condition	Expected Correct	Guess Correct	Adjusted Correct	Mistake	Unexpected Incorrect
GPi	41	42	35	20	29
dACC	31	34	28	22	26

2.5 Data Transfer from Spike2 to MATLAB

Spike2 was the software used to acquire the data from the IED task and was the first software used for data processing. There are different view types including data-based views, text-based views, output sequencer views, grid views, external views, and others (Cambridge Electronic Design Limited, 1988). For this data set, since we were visualizing electrical activity from DBS electrodes, the data-based view type was used. Within the data-based view there are three types of data views including time views, result views, and XY views. We used the time view because this display allows for data to be viewed that

was being sampled by spike2. The time view data types are generally saved or imported as .smr files which is a 32-bit times format file that holds data for individual channels in blocks. Original data files were saved in this format and for this reason Spike2 was initially used to open/access the files which were then marked according to the different types of correct and incorrect trials.

2.6 Data Processing with MATLAB & EEGLAB: Loading Data

The main source of processing done in MATLAB was using the EEGLAB toolbox (Delrome & Makeig, 2004; The Mathworks Inc, 2022). This toolbox in MATLAB helps process continuous and event-related electrophysiological data including EEG, MEG, and LFP data (Delrome & Makeig, 2004). This toolbox can perform independent component analyses (ICA), time/frequency analyses, artifact rejections, event-related statistics, as well as data visualization of the averaged single-trial data. EEGLAB was the toolbox of choice as it is extremely user friendly offering an interactive graphic user interface (GUI) and compatible with various software's including Linux, Unix, Windows, and Mac OS X. Even though this file format is supported by MATLAB, to open these files in EEGLAB, additional plugins were required. The very beginning steps of this project involved spending time learning the best method by which the data files could be opened in EEGLAB to be able to perform the analyses needed. As different plugins and functions were used, different error codes were produced that had to be resolved before the files were successfully opened. The following methods were used to open the data files:

1) Using the File-IO interface → This is an extension of the Fieldtrip toolbox and allows any file format type that is supported by fieldtrip to be opened within EEGLAB (Delrome & Makeig, 2004). This was attempted first because fieldtrip directly supports various file formats including .smr files from Spike2. However, when using this plugin, an error code was generated.
2) Using File-IO interface with Neuroshare → Neuroshare is a software that allows more flexibility with file formats of neurophysiological data (Bergel et al., 2005). Even though Neuroshare was

previously used in the lab alongside the File-IO interface to open .smr files within EEGLAB, this approach also generated error codes and did not work as a means of opening the files.

3) ASCII/float file or MATLAB array → Since the file-IO interface did not allow the files to open within EEGLAB, and .mat files are undoubtedly compatible with MATLAB, the .smr files were individually exported as a .mat file, a binary data file that stores workspace variables (The Mathworks Inc., 2022). This function allows .mat files to be directly imported within EEGLAB. This method also resulted in error codes. Using this same method, basic lines of codes were written to save the file as a MATLAB variable instead of directly opening the .mat file. The following code was used "mydata=load(-'mat', 'your_file.mat'). This loads the raw data into a MATLAB structure which can then be saved into a MATLAB variable by assigning it to a variable "myeeg=mydata.eeg". When this variable has the given data saved, in EEGLAB the data can be loaded by clicking on the ASCII/float file or MATLAB array option. Inside this option import MATLAB variable can be selected and "myeeg" would be typed to open the data within EEGLAB. This approach also generated error codes.
4) Other downloads → After examining the various plugins that EEGLAB offers, the Spike2 EEGLAB plugin was downloaded (Delorme & Makeig, 2004). This plug-in allows the .mat files made by Spike2 to be opened in the format compatible with EEGLAB. This plugin was successful in opening our datasets and was subsequently used to open all the datasets used for this project. It requires a download into the plugin folder within the EEGLAB download folder. Once saved there, within the EELAB toolbox the following series of steps are followed to open the file: file > import data > Using EEGLAB plugins and functions > From Spike2 MATLAB file (.mat). This will allow .mat files exported from Spike2 to be loaded within the EEGLAB GUI.

2.7 Data Preprocessing with MATLAB & EEGLAB:

When data was first imported into EEGLAB, it was epoched. Epoching is an essential step for continuous time locked data such as the dataset we are working with. Since particular events happen at specific time points, extracting data relevant to those time points of interest is an important preprocessing step (Delorme & Makeig, 2004). This was done in the EEGLAB toolbox by selecting tools > extract epochs > Epochs limits [start, end] in seconds > -0.5s, 3s. This selection encompasses the entire duration of the trials so that all aspects can be examined including the start of the visual stimulus on the screen, the motor action of reaching for the screen, the tactile stimuli of touching the screen, and the auditory stimulus of feedback (Figure 3). All data files were re-sampled to a frequency of 512Hz. After epoching and re-sampling, the data was re-saved as a .set file which is the most compatible file type with EEGLAB and the file type that EEGLAB intrinsically produces. Another important data processing step was the removal of basic noise in the signals. EEGLAB has an intrinsic add-on called cleanline which helps to remove baseline noise. The most common type of noise found in signals has to do with powerline interference (Leske & Dalal, 2019). This noise usually appears around the 50Hz to 60Hz frequency range as this is the frequency of the AC current. There are various methods that can be used to remove this noise such as a notch filter which aims to cut out a particular frequency range. This method is usually not preferred as it can create distortions in the signal at other frequencies. Cleanline in EEGLAB has been developed to resolve this issue while filtering this noise. For this reason, Cleanline was used to remove the 50-60Hz noise. It operates by using a regression-based approach that aims to subtract the frequency of choice from the dataset. In addition to removing baseline noise, for dACC patients an additional filtering step was applied. The dACC data had a DC offset present which sometimes occurs when a signal is converted from an analog signal to a digital signal (Drongelen, 2018). Due to a DC offset, the signal will be offset from the baseline value and may not be amplified. To correct for this, the following line of code was used which helps remove the DC offset and recentre the data to a baseline of 0:

"EEG.data=EEG.data-repmat(mean(EEG.data,2),[1 EEG.pnts 1])". This method removes the DC offset by subtracting the data by the mean of each epoch which is one of the best methods used to remove DC offset (Campbell, 2011). Lastly, all data files were bandpass filtered from 0.5-150Hz to obtain cleaner signals.

Standardization of data is a common statistical practice that puts data on the same scale allowing better comparison between different datasets (Junod & Wietlisbach, 1979). Usually when data is being analyzed, different means of the dataset are being compared. There are various methods that can be used to standardize a dataset. For this dataset, the z-score method was used. A z-score is calculated by taking the difference between the mean and a datapoint and dividing it by the standard deviation of that datapoint. This gives a score of how far each data point is from the mean of the dataset in standard deviation. Since all the data is one scale, different variables can be compared. The resulting data will have a mean of 0 with a standard deviation of 1. A simple line of code: N=normalize(A) was used within MATLAB to standardize the data. The normalize command within MATLAB returns the vector wise z-score of the dataset 'A' with a centre mean of 0 and standard deviation 1. Each dataset was opened within EEGLAB first, then the code line N=normalize (EEG.data) was used since the dataset is saved within the EEG.data variable. Once this was done, the line EEG.data=N was used to overwrite the original dataset with the newly normalized dataset. The new standardized dataset was saved and used for further analysis.

2.8 Data Extraction with EEGLAB: Study Function

To conduct various types of time-frequency analyses, the study function within the EEGLAB toolbox was used. This function allows multiple data files to be opened simultaneously for analysis. To create a study, the create a study option was clicked under the file tab. Browse for datasets was selected and, in the pop-up window, all relevant datasets to be compared were uploaded. Numbers were assigned

to each participant and data files so that all the same participants were numbered the same and the datasets part of the same condition were numbered the same. For example, all data corresponding to participant 1 was given a '1' in the subjects' column. All data corresponding to the adjusted correct (one specific condition) was given a 1 for all participants in the conditions column. This function within EEGLAB allows an experimental study to be created so that data from multiple participants in various conditions can be compared together producing various visual and statistical outputs. For this project, the study feature was used mainly to create event-related spectral perturbation (ERSP) images. It is important to note that all patients had six recording channels: RM1, RM2, RM3, LM1, LM2, LM3. The RM or LM correspond to the motor nuclei on the right and left side of the brain respectively. The numbers 1-3 indicate the recording site on the electrode. 1 represents the inner most recording site and 3 refers to the outermost recording site. For the purpose of this thesis only data recorded from LM1 was shown. The reason for this is that all patients were right-hand dominant, so we were interested in the left side of the brain (i.e., the dominant side). The first recording site was chosen because it is the part of the electrode that is closest to the brain region of interest, likely yielding the most reliable results.

2.9 General Theoretical Exploration of Signal Processing Techniques Used in The Project

2.9.1 The Event Related Potential (ERP)

An event-related potential is a means of capturing both sensory and cognitive processes (Sur & Sinha, 2009). At the basis, ERPs are small voltages generated in the brain in response to specific events or stimuli. Since ERPs are time locked to sensory, motor, or cognitive events, they provide a means of studying physiological correlates of mental processes. They generally represent the summarized electrical potentials of neurons that fire synchronously. For this reason, an ERP is unable to resolve activity at the individual neuron level (Woodman, 2010). In practice, ERPs are created when potentials that are time-locked to an event and recorded on multiple trials are averaged together, extracting small amplitude

changes present in each trial. The ERP will generally be seen with peaks and troughs representing changes in voltage during a trial. ERPs can be further analyzed by examining their component waveforms. There are many standard ERP components that are present for given cognitive or sensory processes. One such example is the C1 component which is a consistent waveform believed to be generated by activity in the primary visual cortex, seen when a visual stimulus is present. ERP components are generally described by some common features including their polarity (positive or negative voltage) and timing. One advantage of the ERP analysis is that it provides a means of continuously measuring changes in voltages to see how the activity of neurons is changing in response to various characteristics such as stimulus presentation and the subsequent response (Makeig et al., 2004; Delorme & Makeig, 2004). It is important to note that an ERP is most informative when there are many trials present because of the significantly small size of an ERP.

2.9.2 Fourier Transform

The two types of analysis that commonly get used within the domain of signal processing include the Fourier (stationary signals) and Wavelet transforms (Bishop, 2011). The Fourier transform itself is used for idealized datasets that are infinite which is usually not the case in real-world applications (Prerau Lab, 2021). For this reason, for finite data, a sub domain of the Fourier transform known as the discrete Fourier transform is used to analyze data. The way by which the discrete Fourier transform is produced is through a specialized algorithm known as the fast Fourier transform (FFT). This is the actual code that is used in analysis to generate the discrete Fourier transform. There are three general outputs that then get produced as a result of the discrete Fourier transform including a spectrum which is the power of each given frequency, a power spectral density graph which is a normalized spectrum, and a spectrogram which shows how the spectrum changes over time giving a time-frequency domain. At the core of the Fourier transform, the aim of this analysis is to take complex waveforms and decompose them into a set

of component trigonometric functions such as sine and cosine waves (Bishop, 2011). A signal at its basis is a combination of various sinusoidal components, so the FFT takes the signal and splits it into the individual components that sum up to make the overall signal (Drongelen, 2018). By doing this we can find the component sine waves which each have their own frequencies and amplitudes. By doing this, the time domain of the signal is changed into a frequency domain giving information about how the frequencies vary within the given data signal. The drawback to the FFT is that it is not able to represent signals that are localized in time and provide the frequencies present along the entire signal. For this reason, the temporal and spatial resolution for this type of analysis is lower (Delorme & Makeig, 2004; Drongelen, 2018). Another drawback to this analysis is that it does not capture abrupt changes in signal or short interval characteristics of oscillations as frequencies that are present over an entire signal are shown (Talebi, 2022).

2.9.3 Wavelet Analysis:

On the other hand, wavelet transforms accomplish a very similar output, however they also tend to show data in the time domain (Talebi, 2022). In other words, they show how the frequency is changing across time and space (Delorme & Makeig, 2004; Talebi, 2022). Wavelet transforms follow the same theory but instead of dissecting the signal into trig functions, these transforms split the signal into multiple wavelets. (Drongelen, 2018; Prerau Lab, 2021). The way that this is accomplished is by first choosing a wavelet of particular size and shape and to multiply that wavelet with the signal across all time and locations of the signal. This gives us a coefficient for the wavelet scale (Talebi, 2022). The advantage of the wavelet analysis is that it can extract spectral and temporal information simultaneously (Talebi, 2022). A combination of these techniques can also be used by adjusting the wavelets factor (Delorme & Makeig, 2004). By adjusting the wavelets factor the analysis can be altered to be in between an FFT and a wavelet transform.

2.9.4 Autoregression

Autoregression is an analysis method that can be used to differentiate signal from noise for nonstationary data (Hong-Zhi et al., 1982; Smith & Kutas, 2014). Autoregression in basic theory is an extension of autocorrelation. When data is collected over time, the error that is present can sometimes be positively correlated with time which can sometimes preclude any trends seen in the data over time. This phenomenon is referred to as autocorrelation (serial correlation) and can sometimes be detected by plotting the model residuals over time. An autoregression model stems off this idea and deals with a time series value that is regressed on previous values from the same time series. The basics of this analysis include forecasting a time series variable of interest (y) assuming that it has a linear relationship with another time series variable (x). Different predictors can be used to estimate and forecast the variable (y). The way that autoregression accomplishes this is by using a target's linear combination of past values to make a prediction about the future values (Dimitriou-Fakalou, 2011; Smith & Kutas, 2014). The autoregression model is referred to as the AR(p) model, where p is the order of the model. This order can be determined via autocorrelative measures by using the autocorrelative function (ACF) to identify how correlated values in a time series are with each other. The ACF plots the correlation coefficient against the lag (the time gap between the values). Once this plot is derived, a partial autocorrelation function can be applied to then determine the correlation between the present value and the residuals of the previous lag. This determines the correlation that cannot be explained by the ACF. Ultimately, these processes help determine the order of the autoregressive model which is an important parameter used in the analysis. Within the context of time series data, the Yule-Walker algorithm is commonly applied to give a parametric spectral estimation by returning the estimated power spectral density (power/rads/sample) (PSD) of a vector x (samples of a discrete-time signal).

The first data chapter of this thesis will focus on using ERSP, ERP, and linear regression analyses. The purpose of the ERSP analysis is to determine power differences in the frequencies present across the whole task between the various conditions of incorrect and incorrect trials. The ERP analysis aims to extract characteristics of the movement potential so they can be analyzed across various levels of surprise using a linear regression model. The second data chapter of this thesis aims to use the Fourier transform and autoregression analysis techniques to examine the spectral amplitude and post-spectral density of cognitively relevant frequency bands (theta, alpha, beta, gamma, and high gamma).

3.1 Results Chapter 1: Exploring the Differences Between Correct and Incorrect Trials

3.1.1. Introduction:

The aim of this first data chapter is to examine the differences between all the various correct and incorrect trials. These trials have been categorized across five dimensions. The first comparisons made are between all correct and incorrect trials to see whether or not the dACC and GPi respond differently to all correct and incorrect trials. The main purpose of this comparison was to reproduce data that has been published from the lab to validate the analytical techniques being used. Weiss et al. (2018) had found that the dACC responded differently to incorrect vs correct trials, where the dACC was more sensitive to the presence of error (incorrect trials). Although the Dystonia and Parkinson's data had been analyzed prior to this project, it was mainly examined within the realm of assessing differences within beta, theta, and gamma frequency bands rather than overall differences between correct and incorrect trials (Gillies et al., 2017). The second type of comparison made consisted of comparing sub types of correct trials with one another to determine whether the dACC or GPi respond differently to different types of correct trials. The third type of comparison that was made consisted of comparing two types of incorrect trials with one another. These last two comparisons are the novel aspect of this project as correct and incorrect trials have not been classified in this manner and evaluated regarding differences in electrophysiology. As mentioned

much of the theoretical foundations for these comparisons comes from work done by Fouragnan et al. (2017). This group was able to find electrophysiological differences for levels of surprise (low, medium, high). Since the level of surprise consisted with differences in electrophysiology, it gives reason to believe that there may be electrophysiological differences in the brain in relation to various types of correct and incorrect trials as they can be associated with varying levels of surprise. These ideas were evaluated with time-series analytical techniques such as ERSP analysis that measures average frequency dynamic changes in spectral amplitude relative to baseline over time and the evaluation of ERP parameters.

3.1.2 Methods:

3.1.2.1 ERSP Images & Statistics

ERSP images were generated using EEGLAB within MATLAB. Even though the toolbox ran the appropriate analysis to produce these images, particular criteria had to be inputted to guide the analysis. One example is the removal of an independent component analysis. This analysis is commonly used for EEG data since the data is collected from the scalp and has poor localization. An independent component analysis is one means of improving the localization of the data but since our data represents local field potentials collected from the brain, localization of the data does not need to be improved. Information about the analysis type was also chosen. We chose to use the fast Fourier transform (FFT) to produce the ERSP images as it is the default recommendation and the most common analysis type to produce ERSP images (Delorme & Makeig, 2004). An FFT analysis is a signal processing method that converts a signal into individual spectral components providing frequency information about a signal (Drongelen, 2018). The FFT is an algorithm that has been optimized as an implementation of the discrete Fourier transformation (DFT). A signal is divided into its frequency components as it is sampled over a period of

time. The frequency components are single sinusoidal oscillations each with their own amplitude and phase at distinct frequencies (Grandchamp & Delrome, 2011).

In order to perform this type of analysis, the sampling rate/frequency is required, and this value represents the average number of samples obtained in one second (samples per second) (Drongelen, 2018). The second parameter that is required is the selected number of samples (block length) which is an integer power to the base of 2. Using these two basic parameters, other parameters can be determined such as bandwidth (fn), measurement duration (D), and frequency resolution (df). Alongside these parameters, one important assumption that is made before applying the FFT is that the sampled signal segment is repeated periodically for an infinite period of time which means that the FFT is only suitable for periodic signals and the sampled signal segment must contain a whole number of periods. If these conditions are not met, a smeared FFT spectrum is created. One method to help with this is to use windowing which creates a signal that begins and ends at amplitude zero which can then be repeated periodically without a hard transition. Overall, this type of analysis is used to create visual outputs of data, in the form of 2-D time-frequency images (Drongelen, 2018; Grandchamp & Delorme, 2011). It is important to note that there are some trade-offs between time and frequency resolution (Delorme & Makeig, 2004; Makeig et al., 2004). If the whole epoch is used as a time window, you can get a good representation of frequencies in the signal but there is less time resolution. On the other extreme, if the FFT is applied to very short time windows, this would then not be useful for detecting ranges of frequencies in the signal because the sample would not be big enough to detect oscillations. This technique is useful because it helps generate an ERSP image that then summarizes frequency on the y-axis along with time in the x-axis. It takes the entire duration of the task and shows the power of particular frequencies and how they change across specific time points. There is a colour bar that represents the power, warmer colours ranging from light green to red showcase an increase in power and

have positive numbers attributed to them whereas cooler colours such as blue show a decrease in power and are associated with negative numbers. The scale bar is in db because it is a ratio of the power in the epoch to the average power in the baseline.

Two types of statistics were used for the ERSP images. The first type was permutation statistics, and the second type was bootstrap statistics. Both these types of tests fall under surrogate tests and are examples of non-parametric statistical tests (Berk, 2021; Holt & Sullivan, 2021). Non-parametric tests have very few assumptions associated with them unlike parametric tests which can only be accurately used if a set list of assumptions is fully met. In this case, it is unlikely that our data meets the normal distribution assumption of parametric tests because the sample size for the dataset is very small Permutation statistics work by estimating the population distribution by calculating various probabilistic permutations which then combine to estimate the population's distribution (Berk, 2021). The calculation of the p-value comes from taking the median of the observed data, the median of the permutations, and then determining which one of the medians from the permutations are more extreme than the observed medians. The proportion of this gives the p-value. There are not any significant differences between permutation and bootstrap statistics except that EEGLAB does not recommend the use of bootstrap statistics when there is paired data being compared as it can overestimate significance (Mischchenko, 2021). For this reason, permutation statistics were originally chosen but to match work done by Weiss et al. (2018), bootstrap statistics were also used. The justification behind using bootstrap is that since there are few participants and fewer trials to analyze, the overestimation of significance is unlikely to have an impact on the interpretation of the data. For types of tests, since multiple comparisons were being made, the false discovery rate (FDR) correction was used. This correction helps to correct for random events that may appear falsely significant (Rouam, 1970). This correction is slightly less conservative than other common correction methods used such as the Bonferroni correction (Stephanie, 2023). Since the dataset

used for these analyses was quite small, a less conservative method is a better approach as the likelihood of finding a significant result is already quite low and subsequently a correction for finding falsely significant results is low as well. The FDR correction takes this point into consideration and corrects for 0.05% of false positives.

3.1.2.2 Linear Regression

The second methodological technique that was used was a linear regression-based analysis. This was used to analyze various ERP parameters across the level of surprisingness categorized based on the Rescorla-Wagner model of reinforcement learning (Figure 9).

The Equation

$$\Delta V = \alpha\beta(\lambda - \Sigma V)$$

Figure 9. The Rescorla-Wagner Equation
This equation shows that the amount of learning (V) that takes place depends on the level of surprise that is present (the difference between what was expected and reality) The alpha and beta coefficients pertain to the salience which ultimately impacts the speed of learning (Rescorla & Wagner, 1972).

This model serves the basis of evaluating the subtypes of correct and incorrect trials categorized in this project. When the surprise was high (i.e., a greater difference between the expected vs actual outcome), a greater number was associated with that condition. When the surprise was low (when the difference between what was expected, and the actual outcome is small) a smaller number was assigned to that condition. There were five conditions for the independent variable of surprise including: expected correct

(surprise =1, low surprise), adjusted correct (surprise =2), guess correct (surprise =3), mistake (surprise =4), and unexpected incorrect (surprise =5). Three specific ERP parameters were extracted including the maximum ERP amplitude, the minimum ERP amplitude, and the ERP amplitude range (the difference between the maximum and minimum ERP amplitude). Excel was used as the graphing software to represent the data, in which a linear regression statistical analysis was conducted to show the strength of the linear relationship between the two variables of interest. Normalized data was used for this analysis. ERP parameters were compared across all six recording channels. Overall, the linear regression analysis yielded an R^2 value which is used to identify significance of a relationship. Unlike other statistical analyses, a linear regression does not directly yield a p-value as it aims to determine correlation between two variables. R^2 values are evaluated in three categories: weak > moderate > strong. A value of 0 represents a correlation of 0 indicating that the two variables of interest are not related in any way. A value of 1 represents a perfect relationship. Usually values in the middle of 0 and 1 are obtained. Values between 0.1-0.4 represent a weak correlation, values from 0.4-0.7 represent a medium correlation, and values above 0.7 represent a strong correlation. There are slight variations that can be found in the categorization of these values but generally the categories stay the same when it comes to evaluating the strength of the correlation.

3.1.3 Results & Discussion:

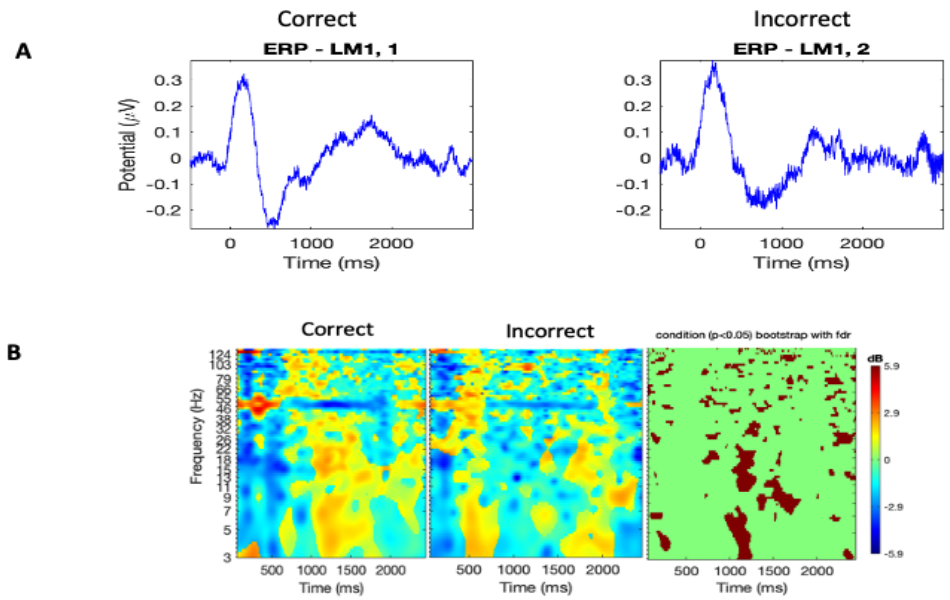


Figure 10. ERP and ERSP Image of Correct vs Incorrect Trials for 5 Dystonia Patients
A) shows the ERP trace for five Dystonia patients for both correct (left) and incorrect (right) trials throughout the task. B) shows the ERSP images of five Dystonia patients with correct trials on the left and incorrect trials on the right. Bootstrap statistics were used with an FDR correction for multiple trials. Brown areas represent statistically significant differences with a p-value <0.05.

The ERSP images as mentioned help visualize the power intensity of various frequencies across time. As a general note, since the ERSP images do show power increases or decreases, this can be observed via the colour present on the image. Red blocks represent higher increases in power whereas dark blues show larger decreases in power. When examining the Dystonia patients, no substantial difference between the two ERPs can be seen (Figure 10). Both ERPs follow the same trend, where the peak occurs around 0ms followed by negative peaks around 1000ms. When looking at the ERSP image for both the correct and incorrect trials, significant differences can be seen within the frequency range 3-40Hz. Bootstrap statistics with an FDR correct was used as mentioned in the methods section with a p

value < 0.05 indicating statistically significant results. These images show power increases and decreases for various frequencies across time. The important conclusion from this analysis is that the differences that are seen between correct and incorrect trials are seen at 1000-1500ms time point for frequencies that have biological significance (theta, beta, and gamma). +500 to +2500ms represents the learning phase of the task so these differences seen are in relation to the learning phase of the task. From this analysis we can see that there are differences between how correct and incorrect trials are processed within the GPi in relation to the learning that occurs during the task.

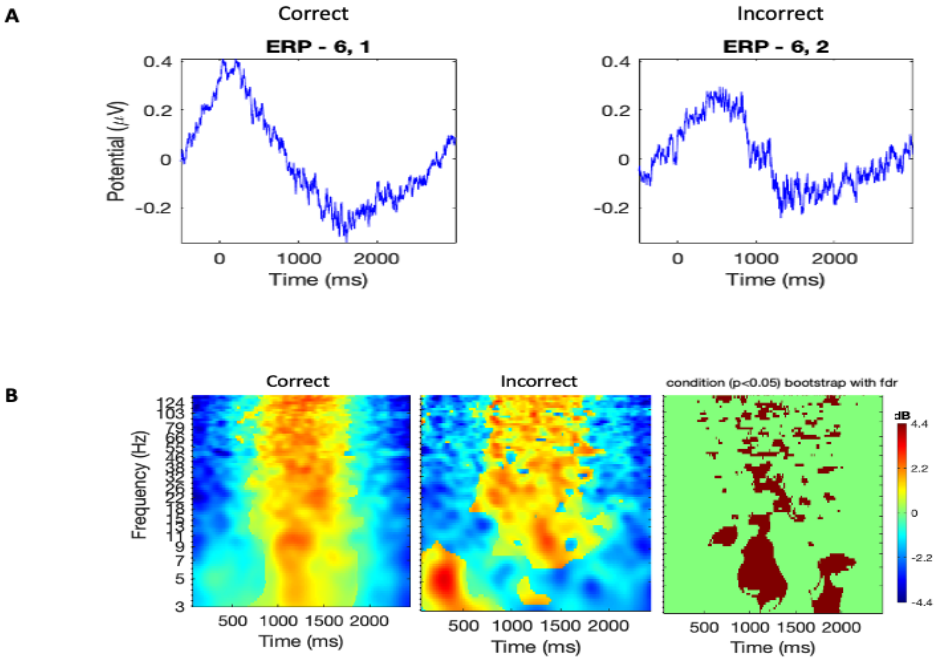


Figure 11. ERP and ERSP Image of Correct vs Incorrect Trials for 4 dACC Patients
A) shows the ERP trace for four dACC patients for both correct (left) and incorrect (right) trials throughout the task. B) shows the ERSP images of four ACC patients which correct trials on the left and incorrect trials on the right. Bootstrap statistics were used with an FDR correction for multiple trials. Brown areas represent statistically significant differences with a p-value <0.05.

For the dACC data, the comparison of correct vs incorrect trials was previously published but it was produced as a means of validating the analytical techniques and re-producing previously published data (Figure 11). In line with Weiss et al. (2018), when correct and incorrect trials were compared, statistically significant differences were found within the frequency range of 3-25Hz around 500-1000 ms and then again at around 2000ms. This is again indicative that the dACC does have different dynamics in the way that it responds to correct vs incorrect trials.

When looking at the data from the Parkinson's patients, it is important to note that this dataset only had two patients and was the smallest dataset of the three. The patients here were tested first with no medications and then again with medications (Figure 12). For all the conditions: meds on correct vs incorrect trials, meds off correct vs incorrect trials, meds on correct vs meds off correct, and meds on incorrect vs meds off incorrect, there were no statistically significant differences found within the ERSP images. This could be due to the fact that there were only two Parkinson's patients as part of this dataset. It could also be due to re-exposure effect as this was the only case where the participants were tested twice on the same task (Palumbo et al., 2021). Since there were no statistically significant results that were found within this dataset and the number of patients was lower than the other two patient sets, no further analysis was done on Parkinson's patients.

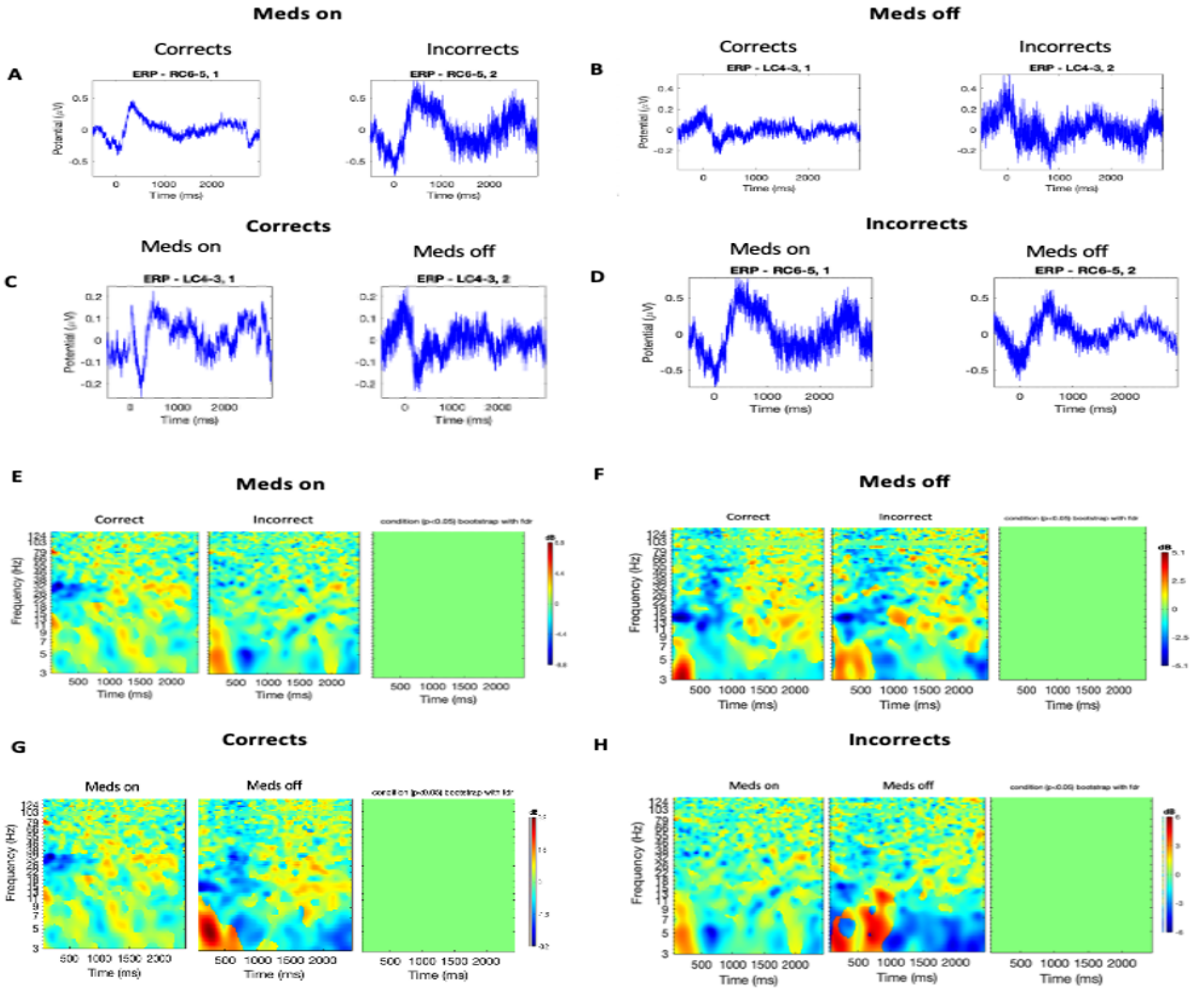


Figure 12. ERP and ERSP Image of Correct vs Incorrect Trials for 2 Parkinson's Patients That were on and Off Medication

A) shows the raw ERP trace for correct (left) and incorrect (right) trials for patients that were on medication. B) Shows the raw ERP trace for correct (left) and incorrect (right) trials for patients that were off medication. C) shows the ERP trace for correct trials for patients that were on medication (left) and off medication (right). D) shows the ERP traces for all incorrect trials for patients that were on medication (left) and off medication (right). E) shows the ERSP image of correct (left) and incorrect (right) trials for patients that were on medication. F) shows the ERSP image for correct (left) and incorrect (right) trials for patients that were off medication. G) shows the ERSP image of all correct trials of patients that were on medication (left) and off medication (right). H) shows the ERSP image of all incorrect trials of patients that were on (left) and off (right) medication. Bootstrap statistics were used with an FDR correction for multiple comparisons with a p-value cut off of 0.05.

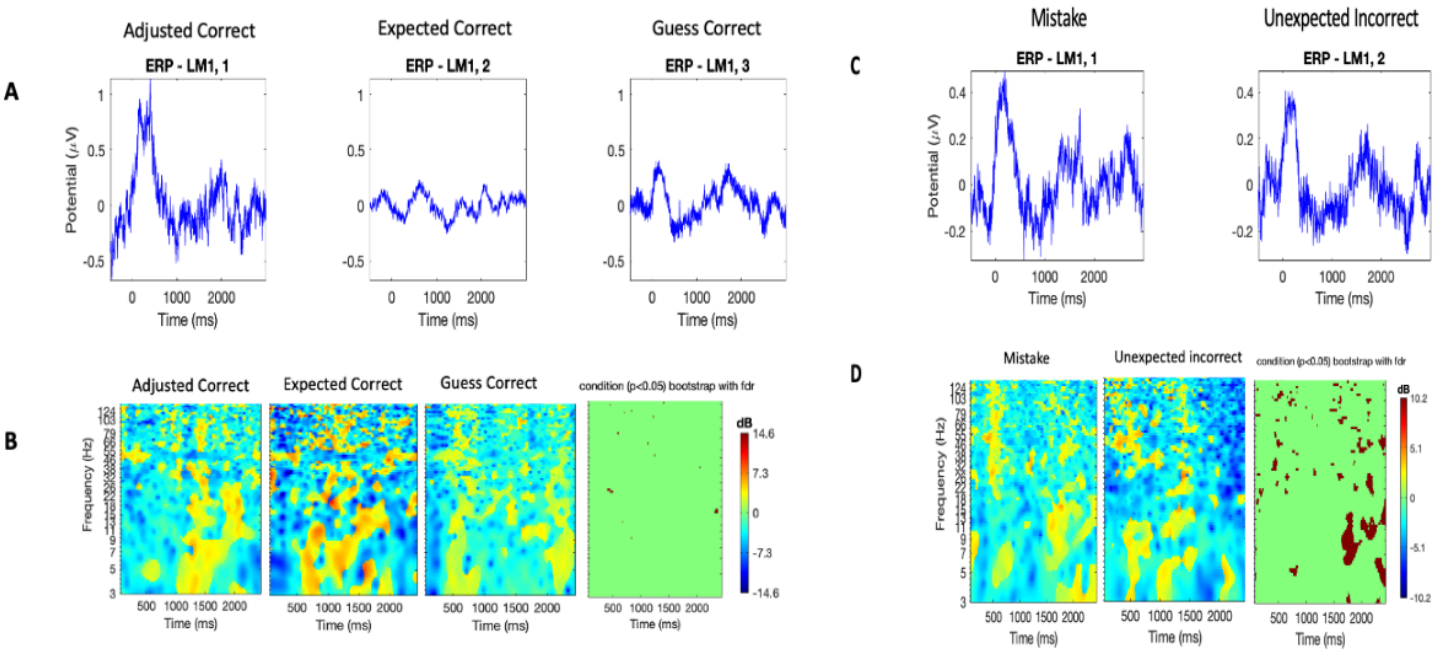


Figure 13. ERP and ERSP images for Five Dystonia Patients Comparing Various Types of Correct and Incorrect Trials

Image A) shows the raw ERP traces for three types of correct trials: adjusted, expected, and guess correct respectively. B) shows the ERSP images for the three types of correct trials. Here significance is determined by comparing each possible combination of all three conditions. Here bootstrapping statistics compares all possible combinations of the conditions to see if there are any differences. Adjusted correct would be compared with expected correct, expected correct would be compared with guess correct, and guess correct will be compared with adjusted correct. If any of these three pairwise combinations have differences, it would show significance where those differences occurred. The only consequence to this is that further statistical analyses would need to be conducted to find out which pairwise combination the differences were coming from. Since there were no significant differences, further analysis was not needed. C) shows the raw ERP traces for the two types of incorrect trials: mistake, and unexpected incorrect. D) shows the ERSP images for the two types of incorrect trials. Bootstrap statistics were used with an FDR correction for multiple comparisons.

Since the dataset with the Dystonia and dACC patients did yield significant differences between the correct and incorrect conditions, further analysis was done to examine different types of correct and incorrect trials. This was one novel aspect of this project as previously mentioned since this type of

classification of correct and incorrect trials has not yet been done before. When looking at the ERSP images for the five conditions for Dystonia patients (expected correct, adjusted correct, guess correct, mistake, and unexpected incorrect), for the correct conditions, the ERP is much larger for the adjusted correct compared to the other two types of correct trials (Figure 13). However, within the ERSP, there are not statistically significant differences between the three types of correct trials (Figure 13). When looking at the comparison of the two types of incorrect trials, the ERP is similar for both the mistake and unexpected error condition. However, within the ERSP image, statistically significant differences can be seen within the 3-25Hz range from 1000ms to 2000ms (learning phase) (Figure 13). When looking at the dACC comparisons, A similar pattern is observed but it is far more robust than the Dystonia patients (Figure 14). The comparison of the correct trials did not yield any significant results, but robust differences were found between the two incorrect conditions. This is not surprising as work in the lab has found that the dACC is responsive to error not correct trials (Weiss et al., 2018). For this reason, the dACC not showing differences in response to types of correct is a result that was expected.

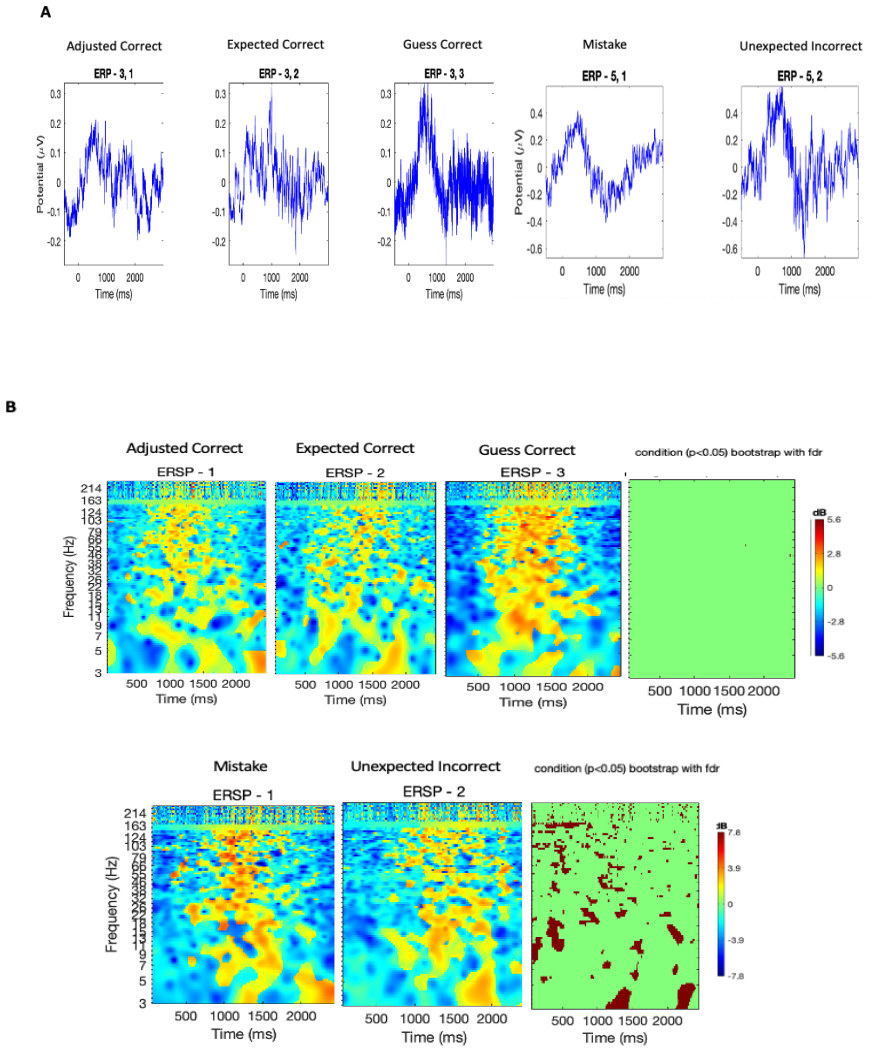


Figure 14. ERP and ERSP images for Four dACC Patients Comparing Various Types of Correct and Incorrect Trials

Image A) shows the raw ERP traces for types of correct and incorrect trials: adjusted, expected, and guess correct mistake, and unexpected incorrect respectively. B) shows the ERSP images for types of correct and incorrect trials. Bootstrap statistics were used with a FDR correction for multiple comparisons. Here bootstrapping statistics compares all possible combinations of the conditions to see if there are any differences. Adjusted correct would be compared with expected correct, expected correct would be compared with guess correct, and guess correct will be compared with adjusted correct. If any of these three pairwise combinations have differences, it would show significance where those differences

occurred. The only consequence to this is that further statistical analyses would need to be conducted to find out which pairwise combination the differences were coming from. Since there were no significant differences, further analysis was not needed.

An ERSP analysis was useful in providing one means of isolating our signal from the surrounding noise and helping to visualize the power of the various frequencies. However, one of the biggest limitations of this analysis is that it comes with a time frequency trade off (Zhang & Koike, 2022). Since the FFT is applied to the signal over different time windows, this by default results in a trade-off between frequency and time resolution. One extreme way to conduct this analysis is to take one big time window as the epoch, which would give high frequency resolution and show represented frequencies very well but no time resolution at all. On the other hand, applying the FFT to shorter time windows gives better time resolution but does not accurately represent the range of frequencies present in the signal because the sample is not large enough to detect the oscillations. The lack of meaningful significance from the ERSP analysis could be due to this limitation as EEGLAB tries to give equal time and frequency resolutions, which could not be strong enough to significantly represent the lower frequencies that we are interested in.

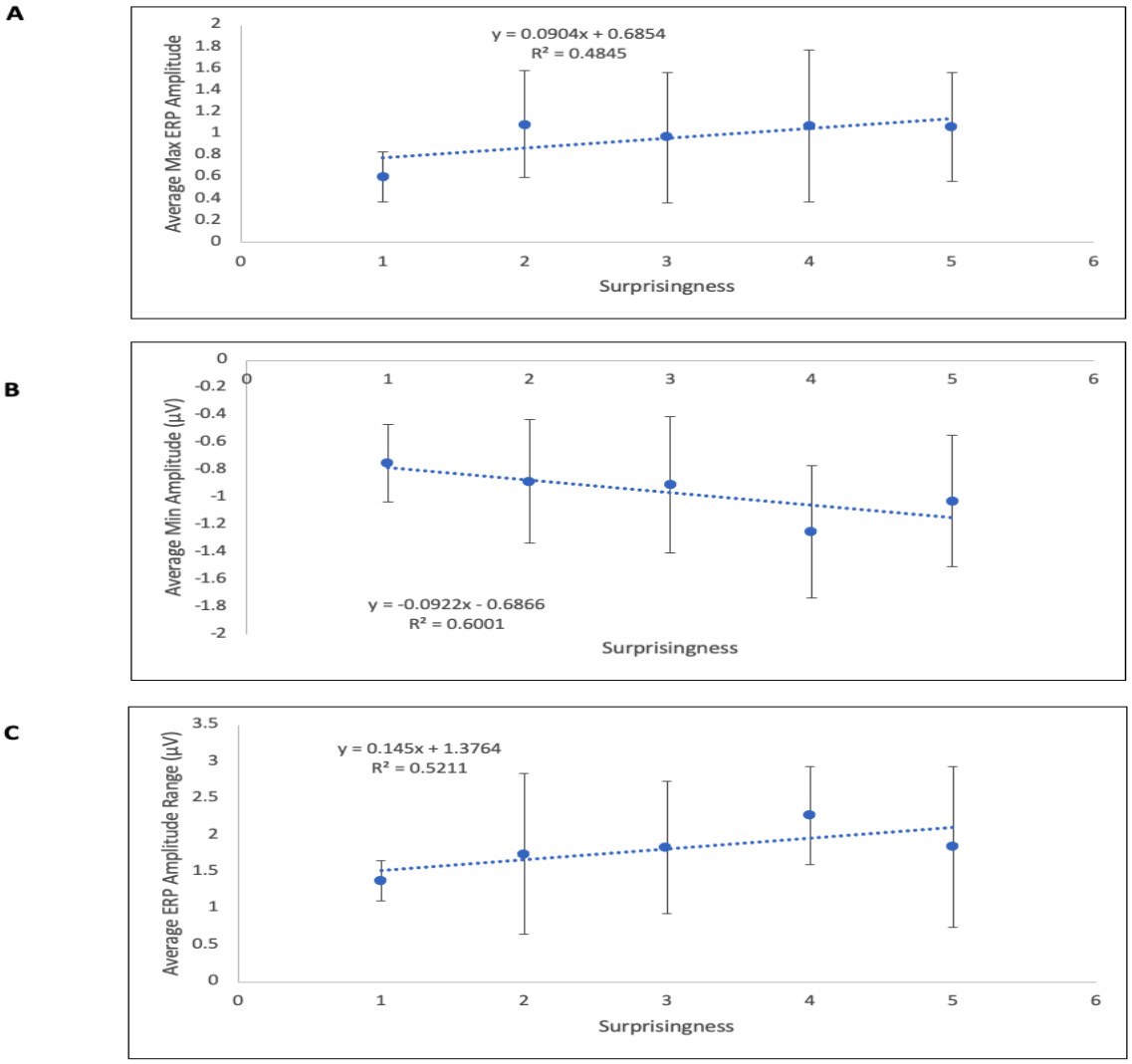


Figure 15. Linear Regression for 5 Dystonia Patients Comparison Various ERP Parameters Across Five Levels of Surprise

The various classifications of correct and incorrect trials were divided into five categories based on their level of surprise. A value of 1 was given for low surprise and a value of 5 was given to the highest surprise outcome. The exact categorization was 1= expected correct, 2=adjusted correct, 3= guess correct, 4= mistake, and 5 =unexpected incorrect. Image A) shows the maximum ERP amplitude averaged across the five patients. Image B) shows the minimum ERP amplitude averaged across the five patients. Image C) shows the average ERP range averaged across the five patients. A linear regression was used as the statistical analysis to evaluate the strength of the relationship between a particular ERP parameter and the level of surprise. Pearson's R was used as a means of evaluating the R^2 values produced.

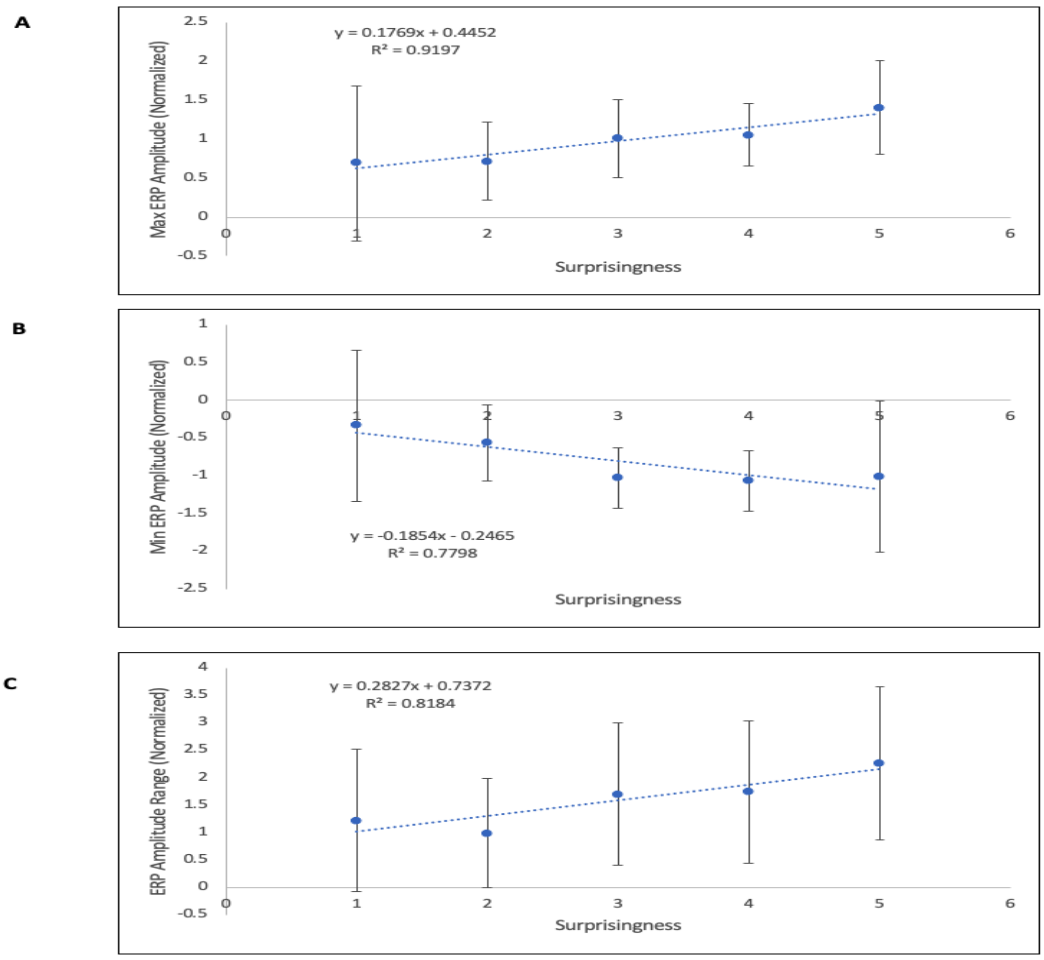


Figure 16. Linear Regression for 4 dACC Patients Comparison Various ERP Parameters Across Five Levels of Surprise

The various classifications of correct and incorrect trials were divided into five categories based on their level of surprise. A value of 1 was given for low surprise and a value of 5 was given to the highest surprise outcome. The exact categorization was 1= expected correct, 2=adjusted correct, 3= guess correct, 4= mistake, and 5 =unexpected incorrect. Image A) shows the maximum ERP amplitude averaged across the five patients. Image B) shows the minimum ERP amplitude averaged across the four patients. Image C) shows the average ERP range averaged across the four patients. A linear regression was used as the statistical analysis to evaluate the strength of the relationship between a particular ERP parameter and the level of surprise. Pearson's R was used as a means of evaluating the R^2 values produced.

Another means of examining differences between the types of correct and incorrect trials was a quantitative evaluation of the ERP parameters to see if there were any differences between the ERPs of the different conditions. A Linear regression analysis was chosen since this analysis finds correlation between two variables. The variables of interest included surprise (1=expected correct trials, 2=adjusted correct trials, 3=guess correct trials, 4=mistake incorrect trials, 5=unexpected incorrect trials) ranging from 1-5 where 1 is the lowest level of surprise and 5 represents the highest level of surprise. This allows us to see whether ERP parameters for the five different conditions have any correlation to the level of surprise present in each condition. For both Dystonia and dACC patients, similar conclusions can be made from the linear regression (Figure 15 & 16). When looking at the max ERP amplitude for both the Dystonia and dACC patients, a general positive trend can be found, where, as the level of surprise increases, the maximum ERP amplitude increases as well. This correlation is of medium significance according to Pearson's R correlation factor. For both patients sets, for the minimum ERP amplitude, a medium negative correlation is found which indicates that as the level of surprise increases, the ERP amplitude decreases becoming more negative. When looking at the ERP amplitude range, there is a positive correlation for both datasets. As the level of surprise increases, the ERP amplitude range increases. All these trends as mentioned have medium strength correlation based on Pearson's R, but it is important to note that the dACC shows a greater correlation in these parameters than the GPi. However, it is important to note that the error bars representing standard deviation are very high. This means that the variability in the dataset is too high for the correlation to be meaningful at this stage of the analysis. All data means overlap within the error bars which means that it is unlikely that the correlation is significant. A solution to this problem would be to reduce the variability of the dataset. The variability of the dataset can be reduced if the sample size of the dataset is increased because the sample means are more likely to be near the true population mean hence reducing the spread of the data points. For this reason, it could be the case that if the sample size is increased that the data may show more reliable trends and results.

An important conclusion from this dataset is that all the statistically significant findings were within the domain of 3-40Hz which represent biologically relevant frequencies. This entire frequency range covers three very important bands including theta (3-8Hz), beta (15-30Hz), and gamma (30-100). These frequencies have cognitive significance, so it is not surprising that the changes that are seen happen to be within these frequency ranges. The biggest limitation with this analysis was that the patient number and trial number was quite small and therefore it was unlikely that there would be a statistically significant result. However, one benefit of this analysis is that you can visually spot differences in power increases and decreases across various frequencies regardless of statistically significant results. Since the Dystonia patients did show distributed small specks of significance and this was the dataset that had more patients and trial numbers, it could further support the need of more participants and trials to find more meaningful significant results.

3.2 Investigating Differences in Correct and Incorrect Trials with Different Epochs Using Fourier Transform & Autoregression

3.2.1 Introduction

This data chapter aims to analyze different epochs of the IED since analysis of the whole task did not yield any substantial results. The goal here is to examine smaller subsections of the tasks that correspond to different cognitive stages and determine whether there are differences within those stages and across stages. Three different epoch lengths were chosen for analysis. The first epoch length consisted of +2700ms to +3200ms which is the time after stimulus presentation pre-movement. This is the phase of the task where patients are decision making, as previous feedback from the trial has been received. The second epoch chosen for analysis is -700ms to +500ms which is termed the peri feedback period of the task. During this time interval, a choice/decision has been made and object selection is made

with feedback occurring immediately. The third epoch chosen was +500ms to +2500ms which occurs post feedback, pre-stimulus presentation. This is termed the learning phase of the task. The first epoch and the third epoch are known not to have ERPs present which makes Fourier transform (for stationary signals) and autoregression (non-stationary signals) the best form of analyses for these epochs. This is because the time window of interest is capturing one single component of the trial and thus, we are not interested in how the frequencies are changing over time but rather are interested in what the amplitude density of particular frequencies are. Although the second epoch does have an ERP (movement potential) the same analysis techniques were chosen to analyze this epoch. This decision was made because these analysis techniques provide a means of quantitative analysis unlike the first data chapter of this project. While running these analyses, the frequency range 0-150Hz was used. Within this frequency range, data was divided into five categories: theta (3-8Hz), alpha (8-15), beta (15-30HZ), gamma (30-100Hz), and high gamma (100-150Hz). This covers the cognitively important frequency ranges relevant to this project.

3.2.2 Methods:

The following scripts were created and used to perform these analyses on MATLAB:

Getting Spectral Amplitude Using The Fourier Transform For All Trials and All Channels

```
function [trial_avg,f] = get_trial_average_fft(EEG)%% Created a function to get the trial averages for the fourier transform
fs = EEG.srate;%% General code for extracting the sampling frequency from EEGLAB dataset
data = EEG.data; %% Extracting the data from EEGLAB loaded file

num_trials = size(data,3);%% Extracting the number of trials present in the dataset, it is the third dimensin of the dataset since the format is channel x times x trials
nFFT = 2^nextpow2(size(data,2)); %% Calculation of the fourier transform of the time data in the dataset
f = (0:(nFFT/2)-1) * (fs/nFFT); %% Calculation of frequencies
num_channels = size(data,1); %%Extracting number of channels from the dataset
all_trial = NaN(num_channels,numel(f),num_trials); %% Creating an array with the number of channels, frequencies, and the number of trials

for c = 1:num_channels %% Creating a loop to calculate the spectral amplitude trial average across frequencies for all six channels
```

```
    for i = 1:num_trials
        trial_data = data(c,:,i);
        %%%%% Compute the FFT
        X_fft = fft(trial_data, nFFT);
        %%%%% Calculate the amplitude spectrum (single-sided)
        X_amp = abs(X_fft(1:nFFT/2)) * 2 / length(trial_data);
        all_trial(c,:,i) = X_amp;

    end
end

trial_avg = mean(all_trial,3);

end
```

Getting Post Spectral Density Using Autoregression For All Trials and All Channels

```
function [trial_avg,F] = get_trial_average_pyulear(EEG,or_d,nfft)%%Creating a function for
autoregression analysis using pyulear function
fs = EEG.srate;%% Extracting sampling frequency from EEGLAB dataset
data = EEG.data; %% Extracting data from EEGLAB

num_trials = size(data,3); %% Extracting number of trials from dataset
num_channels = size(data,1);  %%Extracting number of channels
if mod(nfft,2) ==0
    num_t = (nfft/2+1);
else
    num_t = (nfft+1)/2;
end
all_trial = NaN(num_channels,num_t,num_trials);
for c = 1:num_channels

    trial_data = squeeze(data(c,:,:));
    %%%%% Compute the Autoregressive power spectral density estimate ,Äî Yule-Walker method
    [Pxx,F] = pyulear(trial_data, or_d,nfft,fs);
    all_trial(c,:,:) = Pxx;


end
```

```
trial_avg = mean(all_trial,3);

end
```

Getting Peak Heights

```
function peaks = get_channel_peaks(all_trial,freqs)%% Creating a function to find peak heights in the analyes
num_channels = size(all_trial,1);
peaks = cell(num_channels,2);
for c = 1:num_channels
   data = all_trial(c,:);
   [peaks{c,1},peaks{c,2}]= findpeaks(data,freqs);
end
end
```

Summary of Peak Heights and Frequency For Various Frequency Bands of Interest

```
function [peak_heights,peak_freqs] = get_freq_band_peaks(peaks,bands)%% Creating a function to summarize peak heights based on frequency for various differentfrequency bands of interest

n_bands = size(bands,1);
n_channels = size(peaks,1);
peak_heights = cell(n_channels,n_bands);
peak_freqs = cell(n_channels,n_bands);
for c = 1:n_channels
   for i = 1:n_bands
      peak_inds = (peaks{c,2} <bands(i,2)) & (peaks{c,2} >=bands(i,1));
      peak_heights{c,i} = peaks{c,1}(peak_inds);
      peak_freqs{c,i} = peaks{c,2}(peak_inds);
   end
end
end
```

Main Script Utilizing All Functions

```
clearvars -except EEG %% clears variables in workspace apart from the EEG dataset
%% Calculate fft and pyulear trial average for all channels
or_d = 5;
nfft_pyulear = 16384;
[trial_avg_fft,f] = get_trial_average_fft(EEG);
[trial_avg_pyulear,F] = get_trial_average_pyulear(EEG,or_d,nfft_pyulear);
%% Calculate the peak heights and locations for the trial averages
peaks_fft = get_channel_peaks(trial_avg_fft,f);
peaks_pyulear = get_channel_peaks(trial_avg_pyulear,F);
%% Get the peak heights and locations for specific frequency bands
bands = [ 3 8;15 30;30 100;100 150];
[fft_peak_heights,fft_peak_freqs] = get_freq_band_peaks(peaks_fft,bands);
[pyulear_peak_heights,pyulear_peak_freqs] = get_freq_band_peaks(peaks_pyulear,bands);
%% Production of Figures
%%transform and autoregression analysis across all 6 channels
figure
subplot(1,2,1)
plot(f,log(trial_avg_fft));
xlim([0,150])
subplot(1,2,2)
plot(F,log(trial_avg_pyulear));
xlim([0,150])
legend('Channel 1','Channel2 ','Channel 3','Channel 4','Channel 5','Channel 6')
```

These scripts were created to perform both the Fourier transform analysis and autoregression analysis, to extract visual graphs of the analysis, and to detect peaks within various frequency bands of interest. For the peaks that were extracted, the amplitude of those peaks were evaluated across selected conditions. Since the linear regression from the previous chapter showed a trend in the five conditions of correct and incorrect trials with ERP parameters in relation to surprise, the two most extreme conditions were chosen for evaluation for this chapter. These two conditions included expected correct trials and

unexpected incorrect trials. The rationale here was that if there are likely to be any differences in relation to the different epochs selected it would be apparent within this comparison. Prism GraphPad was used as the statistical software to construct graphs and obtain statistical values. For all datasets, a two-tailed Mann-Whitney U test was used which is the non-parametric equivalent of the parametric unpaired t-test. The reason the nonparametric version was used is because the distribution of the dataset is unknown, and due to the low number of patients it is unlikely that the data set represents a normal distribution. Example graphs are shown in the results section as well as data tables summarizing the U value as well as the exact p value. $P<0.05$ was used as an evaluation of significance. An FDR correction was used for multiple comparisons of trials and patients.

3.2.3 Results & Discussion

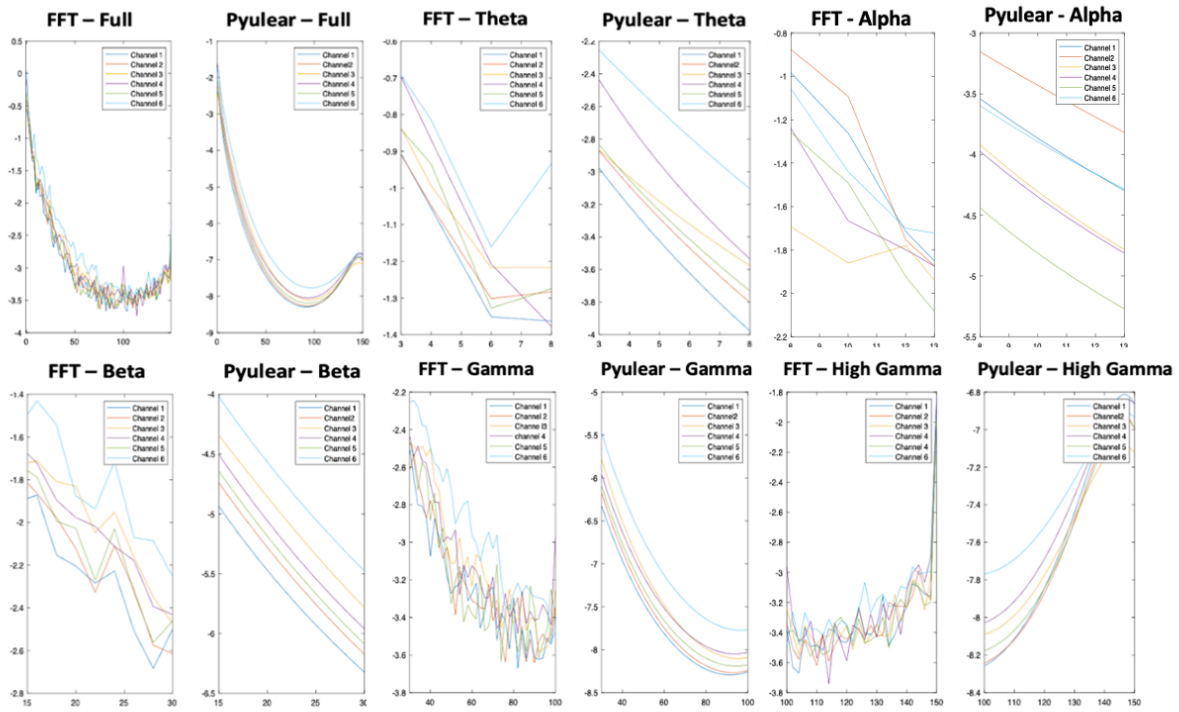


Figure 17. Example Figure of Fourier Transform and Autoregression Analysis
This is the visual output of the Fourier transform and autoregression analysis that were performed for all GPi patients and dACC patients. There were five frequency bands of interest that were looked at including theta (3-8Hz), alpha (8-13 Hz), beta (13-30 Hz), gamma (30-100Hz), and high gamma (100-150Hz). The figures with FFT represent the output for the Fourier transform which show the various amplitudes that were found within a given frequency band across patients and trials. The figures with pyulear show the output of the autoregression analysis which show the post spectral density found in the given frequency bands. This figure is meant to show a sample of the data that was analyzed for this data chapter.

For this data chapter, the goal was to analyze three different cognitive components present in each trial for various cognitively important frequencies (Figure 17). Specifically, the theta (3-8Hz), alpha (8-13 Hz), beta (13-30 Hz), gamma (30-100Hz), and high gamma (100-150Hz) frequencies were evaluated for the decision making phase, the peri feedback phase, and the learning phase of each trial. Trials were first

averaged and then the various amplitudes and post spectral density values were found for all frequency bands for two of the most extreme conditions of surprise (expected correct trials and unexpected incorrect trials). When looking at the decision-making phase for GPi data, no peaks were detected within the theta frequency band. For all other frequency bands, no significant differences were found between the expected correct and unexpected incorrect condition when it came to peak amplitude and post spectral density (Figure 18).

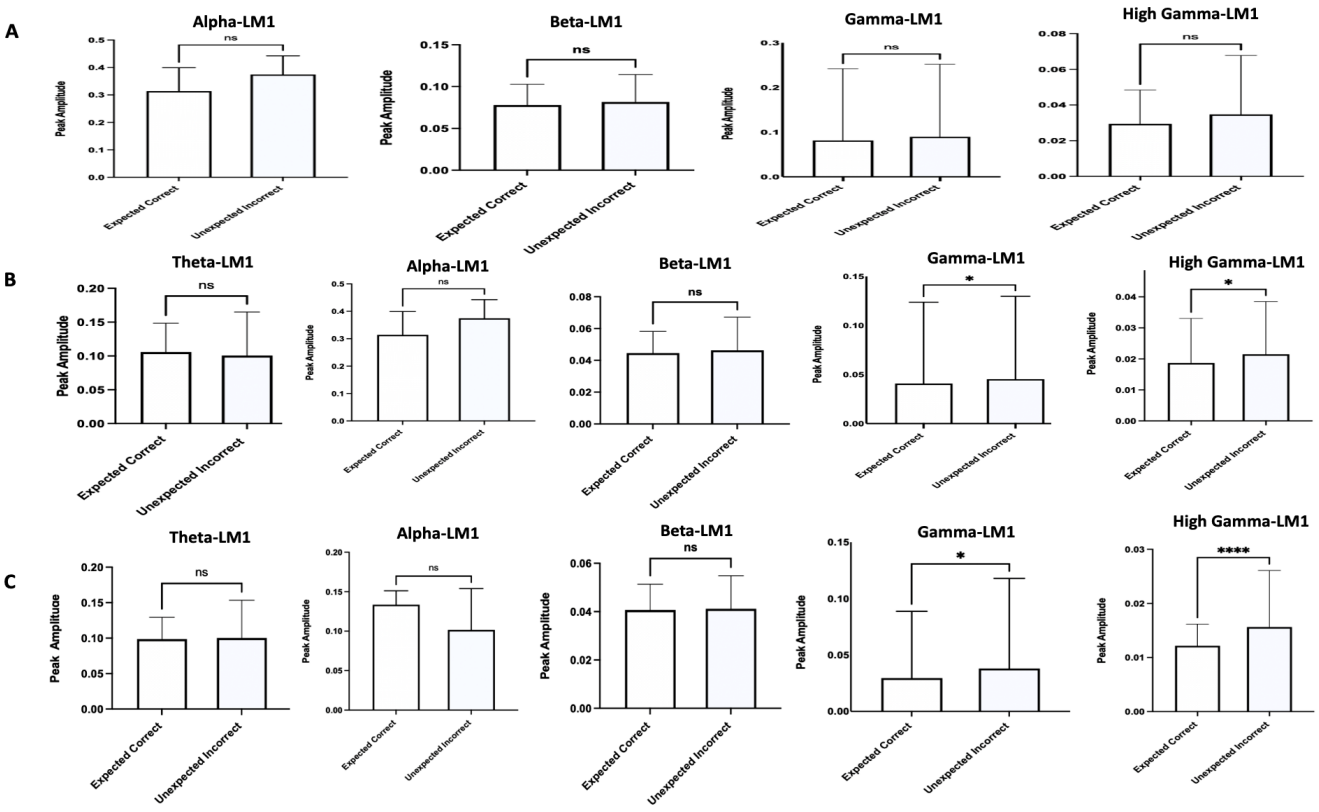


Figure 18. Statistical Comparison of Expected Correct and Unexpected Incorrect Trials For the Decision-Making Phase, the Peri Feedback phase, and the Learning Phase in the GPi
This figure shows three cognitive components of each trial in the IED task. Figure A) represents the decision-making phase of the trial, figure B) represents the peri feedback phase of the trial, and figure C) represents the learning phase of the trial. This is a graphical representation of the average peak amplitude that was found for each of the five frequency bands of interest (theta, alpha, beta, gamma, and high gamma) across five patients and trials. Only the expected correct and unexpected incorrect trials were chosen for comparison as these are the two most extreme conditions. Ns refers to comparisons that were not significant after performing the Mann-Whitney U nonparametric test and applying the FDR correction. One star refers to significant comparison with $P < 0.05$. Two stars or more refer to $p < 0.01$. All data is present from recording channel 1 (LM1). This channel was chosen for analysis as it is likely representing activity closest to the brain region of interest in the dominant side of the brain. Exact p-values and U values can be found in Table 2 alongside the results for the autoregression analysis. Graphs for the autoregression analysis were not shown since the analysis did not find any peaks in the majority of frequency bands.

Table 2. The Summary Statistics Values for the Fourier Transform and Autoregression Analysis for all Trial Components for Five Dystonia Patients (GPi) From LM1.
Bolded values represent statistically significant results. P-values have been corrected using the FDR correction for multiple comparisons. N/A refers to analyses that could not be performed due to a lack of peaks being detected in the given frequency band of interest.

Condition	Theta	Alpha	Beta	Gamma	High Gamma
Fourier Transform (FFT) Decision-Making	N/A	U=76, P=0.9786	U=69, P=0.9095	U=1204, P=0.5242	U=785, P=0.4937
Autoregression (Pyulear) Decision-Making	N/A	N/A	N/A	N/A	N/A
Fourier Transform (FFT) Peri Feedback	U=126, P=0.2369	U=2, P=0.800	U=894, P=0.9618	**U=21247, P=0.0268**	**U=8826, P=0.0483**
Autoregression (Pyulear) Peri Feedback	N/A	N/A	N/A	N/A	N/A
Fourier Transform (FFT) Learning phase	U=91, P=0.8372	U=27, P=0.156	U=1047, P=0.8867	**U=17238, P=0.0104**	**U=6856, P<0.0001**
Autoregression (Pyulear) Learning Phase	N/A	N/A	N/A	N/A	N/A

This is consistent with the results found in the ERSP analysis of data chapter one as no changes in frequency power were seen in the epoch times relating to the decision-making phase of the trial. This does suggest that the GPi may not play a functional role when it comes to the level of surprise present during the decision-making phase. During the peri-feedback phase and the learning phase of the trial, when participants have received feedback from the previous trial and are processing the feedback prior to the next trial, the GPi only shows significant differences in the peak amplitudes for the gamma and high

gamma frequency bands (Figure 18). This difference is interesting as the gamma/ high gamma frequencies are very commonly linked to arousal, learning, memory, and long-term potentiation (Gillies et al., 2017; Jenkinson et al., 2013). Peak amplitudes for the unexpected incorrect condition are higher than the expected correct conditions (Figure 18). This can indicate that a greater presence of gamma/high gamma is required in the incorrect conditions to enhance learning, memory, and arousal to prevent this error from occurring in future trials. This suggests that the GPi does respond to either the surprise or the valence of an outcome, particularly aiding in enhancing the memory of incorrect trials over correct trials or enhancing the memory of more surprising outcomes over less surprising outcomes. One limitation of comparing expected correct and unexpected incorrect trials is that they differ both in their valence and surprise components. For this reason, whether the GPi is responding to valence or surprise cannot be concluded. It still highlights the role of the GPi in the context of cognition, as both these parameters are cognitive parameters.

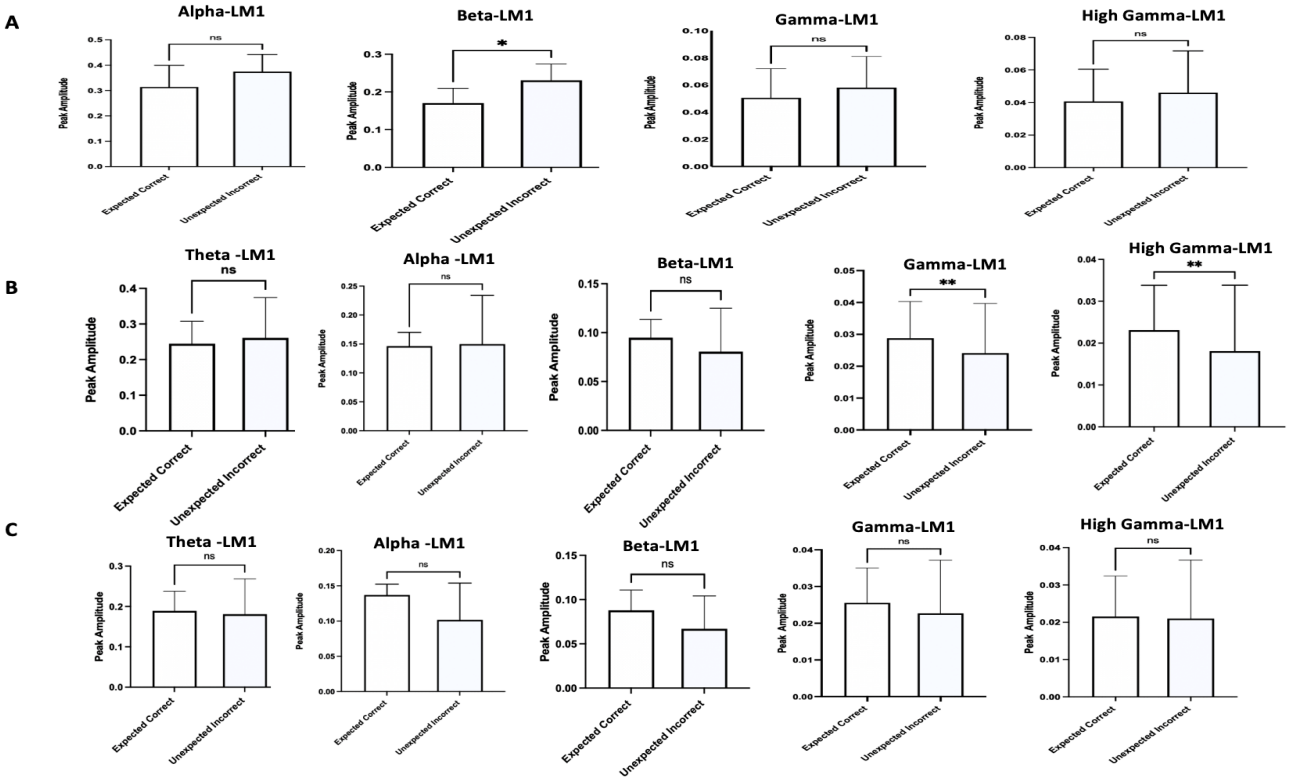


Figure 19. Statistical Comparison of Expected Correct and Unexpected Incorrect Trials For the Decision-Making Phase, the Peri Feedback phase, and the Learning Phase in the dACC
This figure shows three cognitive components of each trial in the IED task. Figure A) represents the decision-making phase of the trial, figure B) represents the peri feedback phase of the trial, and figure C) represents the learning phase of the trial. This is a graphical representation of the average peak amplitude that was found for each of the five frequency bands of interest (theta, alpha, beta, gamma, and high gamma) across four patients and trials. Only the expected correct and unexpected incorrect trials were chosen for comparison as these are the two most extreme conditions. Ns refers to comparisons that were not significant after performing the Mann-Whitney U nonparametric test and applying the FDR correction. One star refers to significant comparison with $P < 0.05$. Two stars or more refer to $p < 0.01$. All data is present from recording channel 1 (LM1). This channel was chosen for analysis as it is likely representing activity closest to the brain region of interest in the dominant side of the brain. Exact p-values and U values can be found in Table 3 alongside the results for the autoregression analysis. Graphs for the autoregression analysis were not shown since the analysis did not find any peaks in the majority of frequency bands.

Table 3. The Summary Statistics Values for the Fourier Transform and Autoregression Analysis for all Trial Components for Four Chronic Pain Patients (dACC) From LM1.
Bolded values represent statistically significant results. P-values have been corrected using the FDR correction for multiple comparisons. N/A refers to analyses that could not be performed due to a lack of peaks being detected in the given frequency band of interest.

Condition	Theta	Alpha	Beta	Gamma	High Gamma
Fourier Transform (FFT) Decision-Making	N/A	U=2, P=0.800	**U=9, P=0.0145**	U=509, P=0.0642	U=342, P=0.4333
Autoregression (Pyulear) Decision-Making	N/A	N/A	N/A	N/A	U=4, P=0.6286
Fourier Transform (FFT) Peri Feedback	U=57, P=0.8718	U=76, P=0.9786	U=652, P=0.0820	**U=13848 P=0.0020**	**U=6367 P=0.0015**
Autoregression (Pyulear) Peri Feedback	N/A	N/A	N/A	N/A	U=2, P=0.5333
Fourier Transform (FFT) Learning phase	U=93, P=0.8562	U=20, P=0.0831	U=589, P=0.8562	U=15119, P=0.2139	U=6971, P=0.3137
Autoregression (Pyulear) Learning Phase	N/A	N/A	N/A	N/A	U=4, P=0.6286

When looking at the data from the dACC, statistically significant differences are found in the gamma/high gamma frequencies within the peri-feedback phase of the trial and in the beta frequency within the decision-making phase of the trial (Figure 19). This is an interesting result because the dACC is known to be a part of the early system when it comes to error detection (Fouragnan et al., 2015; Fouragnan et al., 2017). With this in mind, the fact that significant differences in the gamma/high gamma frequencies are found within the peri feedback component of the trial are not surprising. This is the initial period where feedback is received and so gamma/high gamma differences in this frequency further support the idea that

the dACC processes information related to error early on. Furthermore, the differences found in the dACC show the opposite of what was found in the GPi (Figure 18 and Figure 19). In the dACC the expected correct trials show a higher amplitude compared to the unexpected incorrect trials. This reversal in gamma/high gamma could therefore be one potential mechanism by which the early system downregulates the late system. Having less gamma/high gamma for unexpected incorrect conditions may be the means by which the activation of the late system is slowed down to promote avoidance learning within the late system (i.e., basal ganglia). Another interesting find is the difference in beta that is seen in the decision-making phase of the trial. Consistent with literature, the dACC is known to update future expectations and this difference during the later decision-making phase could be important for that process.

Aside from the frequency band evaluation, another important aim of this chapter was to use two techniques (Fourier transform and autoregression). When comparing the two techniques, a disadvantage to using the Fourier transform was that it was less selective in detecting peaks within the frequency. This makes it likely that peaks that are likely to be insignificant are part of the analysis. On the other hand, the use of autoregression seemed to generate highly selective peaks to the extent where much of the analysis either could not be conducted or was conducted with a very small dataset. This is why graphs for the autoregression were not presented in the thesis. The lack of results from the autoregressive analysis do suggest that it may not be an ideal analysis technique for this dataset. One reason that autoregression may not have been an ideal analysis technique could be because the autocorrelation coefficient may have been less than 0.5 (Turing, 2022). Autoregression only works accurately when there is an autocorrelation coefficient of 0.5 or more. This is because it relies on past values to predict future values. It could be the case that there were not enough trials to use this model reliably as both these conditions only use a small subset of the overall trials or that the data did not model a linear relationship. It is important to note that

looking at peak amplitude or post-spectral density are only two out of many ways that this data could be quantified. A better approach could be to look at frequency power which is similar to the ERSP analysis but to narrow it down to the specific frequency bands of interest. Looking at differences in power could be a more informative analysis then looking at the raw data computed from the Fourier and autoregression analysis. In the future, even channel differences can be looked at as well as the non-dominant side of the brain to see if there are any laterality differences in these frequencies of interest.

4. Conclusion:

This project utilized several analytical techniques including ERSPs, ERPs, linear regression, Fourier transform, and autoregression to examine differences between types of correct and incorrect trials. As a summary, results from this project not only validate that the dACC is indeed sensitive to differences between correct and incorrect trials, but also show that the GPi shows differences between correct and incorrect trials. Both the dACC and the GPi seem to be insensitive to types of correct trials. In addition, when evaluating the types of correct and incorrect trials across their level of surprise, general trends were seen in relation to the ERP amplitude increasing as the level of surprise increased. Having evaluated this idea further, when examining different aspects of the IED task, differences between the two most extreme levels of surprise can be seen within various cognitively relative frequency bands.

Important limitations of this study include the limited number of trials. Since this project divided correct and incorrect trials into identifiable sub trials, the actual number of trials used for analysis were quite low. This makes detecting signal from noise more difficult which is the main goal of signal processing and the ultimate goal within the realm of electrophysiological analysis. This problem can be solved by either getting more participants (which is not always feasible) or by using a different version of the task that contains more sub trials. There are several other cognitive tasks that can be used instead

which may highlight surprise conditions better than the IED task. Reversal learning tasks would be beneficial to use in the future as they specifically allow for surprise to be monitored in greater detail. This can be seen in the work done by Fouragnan et al. (2017). They used a probabilistic reversal learning task in which participants had to identify symbols with the highest reward probability. After learning had occurred there would be a reversal phase where the highest reward probability would unexpectedly switch to a previously low probability symbol. Since probability is mentioned across a scale, this would allow finer manipulation of the element of surprise as seen in their paper. This paper also utilized more complex ways of modelling surprise which should be an aim of future work. The Rascorla-Wagner model as used in this paper is a simple model that explains pavlovian conditioning learning but there are other models such as the reinforcement learning algorithm that deals with predicting RPEs (important for more accurately isolating surprise). Using a task like this would also increase trial numbers. In addition to a different task being utilized, different cognitive parameters can also be evaluated such as reaction time. For this project trials were classified to form subgroups of correct and incorrect trials, but trials can also be classified according to reaction time. Similar analyses can be performed to examine the activity of these areas in relation to the cognitive parameter of reaction time.

In conclusion, this project had several noteworthy aspects including the categorization of correct and incorrect trials into subtypes, categorization of these sub-trials based on surprise, the utilization of deep brain data rather than scalp-based EEG signals, and the examination of sub-components of the IED task. Although Weiss et al. (2018) and Keogh et al. (2022) did examine differences between correct and incorrect trials within the dACC, they had not subclassified the trials beyond these two dimensions. Work done by them also did not use analysis techniques like autoregression and the Fourier transform peak detection that was used in this project. Their work also did not thoroughly examine the different components of the IED task in relation to the pre-movement and post-feedback period encompassing the

learning and decision-making phase. Furthermore, when these areas of the brain have been studied in the context of reward and error learning, the data is usually from fMRI or EEG studies rather than deep brain local field potentials. By examining the dACC and the GPi from a cognitive perspective in this more novel manner, we were able to find evidence to suggest that these nuclei indeed serve a cognitive role in how they respond to reward and error, specifically with regards to the level of surprise present.

References

Akkal, D., Bioulac, B., Audin, J., & Burbaud, P. (2002). Comparison of neuronal activity in the rostral supplementary and cingulate motor areas during a task with cognitive and motor demands. *The European journal of neuroscience*, *15*(5), 887–904. https://doi.org/10.1046/j.1460 9568.2002.01920.x

Amiez, C., Joseph, J. P., & Procyk, E. (2005). Anterior cingulate error-related activity is modulated by predicted reward. *The European journal of neuroscience*, *21*(12),3447–3452. https://doi.org/10.1111/j.1460-9568.2005.04170.x

Amiez, C., Joseph, J. P., & Procyk, E. (2006). Reward encoding in the monkey anterior cingulate cortex. *Cerebral cortex (New York, N.Y. : 1991)*, *16*(7), 1040–1055. https://doi.org/10.1093/cercor/bhj046

Amon, A., & Alesch, F. (2017). Systems for deep brain stimulation: Review of technical features. *Journal of Neural Transmission*, *124*(9), 1083–1091. https://doi.org/10.1007/s00702-017-1751-6

Asemi, A., Ramaseshan, K., Burgess, A., Diwadkar, V. A., & Bressler, S. L. (2015). Dorsal anterior cingulate cortex modulates supplementary motor area in coordinated unimanual motor behavior. *Frontiers in human neuroscience*, *9*, 309. https://doi.org/10.3389/fnhum.2015.00309

Bergel, T., Gruner, C., Guillory, S., Loffler, H., Plummer, T., Reina, T., Stengel, C., Korver, K., Wiggins, H., Wilson, W. (2005). *Neuroshare* [Computer Software]. https://neuroshare.sourceforge.net/download.shtml

Berk, M. (2021). *How to use permutation tests*. Medium. https://towardsdatascience.com/how-to-use-permutation-tests-bacc79f45749

Bishop, D. (2011). *Simplified introduction to time-frequency analysis in EEGLAB*. Bishop_techbits.http://bishoptechbits.blogspot.com/2010/07/simplified-introduction-to-time.html

Blanchard, T. C., & Hayden, B. Y. (2014). Neurons in dorsal anterior cingulate cortex signal postdecisional variables in a foraging task. *The Journal of neuroscience : the official journal of the Society for Neuroscience*, *34*(2), 646–655.https://doi.org/10.1523/JNEUROSCI.3151-13.2014

Blenkinsop, A., Anderson, S., & Gurney, K. (2017). Frequency and function in the basal ganglia: the origins of beta and gamma band activity. *The Journal of physiology*, *595*(13), 4525–4548. https://doi.org/10.1113/JP273760

Boccard, S. G., Fernandes, H. M., Jbabdi, S., Van Hartevelt, T. J., Kringelbach, M. L., Quaghebeur, G., Moir, L., Mancebo, V. P., Pereira, E. A., Fitzgerald, J. J., Green, A. L., Stein, J., & Aziz, T. Z. (2016). Tractography Study of Deep Brain Stimulation of the Anterior Cingulate

Cortex in Chronic Pain: Key to Improve the Targeting. *World neurosurgery*, *86*, 361–70.e703. https://doi.org/10.1016/j.wneu.2015.08.065

Brittain, J. S., Sharott, A., & Brown, P. (2014). The highs and lows of beta activity in cortico-basal ganglia loops. *The European journal of neuroscience*, *39*(11), 1951–1959. https://doi.org/10.1111/ejn.12574

Brown, J. W., & Braver, T. S. (2005). Learned predictions of error likelihood in the anterior cingulate cortex. *Science (New York, N.Y.)*, *307*(5712), 1118–1121. https://doi.org/10.1126/science.1105783

Cai, X., & Padoa-Schioppa, C. (2012). Neuronal encoding of subjective value in dorsal and ventral anterior cingulate cortex. *The Journal of neuroscience : the official journal of the Society for Neuroscience*, *32*(11), 3791–3808. https://doi.org/10.1523/JNEUROSCI.3864-11.2012

Cambridge Electronic Design Limited. (1988). *Spike2 for Windows* (Version 7.12) [Computer Software]. https://ced.co.uk/img/Spike7.pdf

Campbell , K. (2011). *[Eeglablist] Calculating Alpha Asymmetry*. [eeglablist] calculating alpha asymmetry. https://sccn.ucsd.edu/pipermail/eeglablist/2011/003821.html

Chudasama, Y., Daniels, T. E., Gorrin, D. P., Rhodes, S. E., Rudebeck, P. H., & Murray, E. A.(2013). The role of the anterior cingulate cortex in choices based on reward value and reward contingency. *Cerebral cortex (New York, N.Y. : 1991)*, *23*(12), 28842898. https://doi.org/10.1093/cercor/bhs266

Cunnington, R., Windischberger, C., Deecke, L., & Moser, E. (2002). The preparation and execution of self-initiated and externally-triggered movement: a study of eventrelated fMRI. *NeuroImage*, *15*(2), 373–385.https://doi.org/10.1006/nimg.2001.0976

Delorme, A., & Makeig, S. (2004). EEGLAB: an open source toolbox for analysis of single-trial EEG dynamics including independent component analysis. *Journal of neuroscience methods*, *134*(1), 9–21. https://doi.org/10.1016/j.jneumeth.2003.10.009

Dimitriou-Fakalou, C. (2011). Yule-Walker Estimation for the Moving-Average Model. *International Journal of Stochastic Analysis*. 2011. 10.1155/2011/151823.

Doll, B. B., & Frank, M. J. (2009). The basal ganglia in reward and decision making. *Handbook of Reward and Decision Making*, 399–425. https://doi.org/10.1016/b978-0-12-374620-7.00019-4

Drongelen, W. van. (2018). *Signal Processing for neuroscientists*. Elsevier, Academic Press.

EEGLAB. (2019). *EEGLAB time-frequency decomposition Part 3: Event related spectralperturbation* [Video].YouTube. https://www.youtube.com/watch?v=9S2CnpJ9cc

Ellis T. L. (2011). Dystonia and the role of deep brain stimulation. *ISRN surgery*, *2011*, 193718. https://doi.org/10.5402/2011/193718

Fan, H., Zheng, Z., Yin, Z., Zhang, J., & Lu, G. (2021). Deep brain stimulation treating dystonia: A systematic review of targets, body distributions and etiology classifications. *Frontiers in Human Neuroscience*, *15*. https://doi.org/10.3389/fnhum.2021.757579

Fouragnan, E., Retzler, C., Mullinger, K., & Philiastides, M. G. (2015). Two spatiotemporally distinct value systems shape reward-based learning in the human brain. *Nature communications*, *6*, 8107. https://doi.org/10.1038/ncomms9107

Fouragnan, E., Queirazza, F., Retzler, C., Mullinger, K. J., & Philiastides, M. G. (2017). Spatiotemporal neural characterization of prediction error valence and surprise during reward learning in humans. *Scientific reports*, *7*(1), 4762. https://doi.org/10.1038/s41598-017-04507-w

Gillies, M. J., Hyam, J. A., Weiss, A. R., Antoniades, C. A., Bogacz, R., Fitzgerald, J. J., Aziz, T. Z., Whittington, M. A., & Green, A. L. (2017). The cognitive role of the globus pallidus Interna; insights from disease states. *Experimental Brain Research*, *235*(5), 1455–1465. https://doi.org/10.1007/s00221-017-4905-8

Grandchamp, R., & Delorme, A. (2011). Single-trial normalization for event-related spectral decomposition reduces sensitivity to noisy trials. *Frontiers in psychology*, *2*, 236. https://doi.org/10.3389/fpsyg.2011.00236

Groiss, S. J., Wojtecki, L., Südmeyer, M., & Schnitzler, A. (2009). Deep brain stimulation in Parkinson's disease. *Therapeutic advances in neurological disorders*, *2*(6), 20–28. https://doi.org/10.1177/1756285609339382

Hayden, B. Y., & Platt, M. L. (2010). Neurons in anterior cingulate cortex multiplex information about reward and action. *The Journal of neuroscience : the official journal of the Society for Neuroscience*, *30*(9), 3339–3346. https://doi.org/10.1523/JNEUROSCI.4874-09.2010

Hayden, B. Y., Heilbronner, S. R., Pearson, J. M., & Platt, M. L. (2011). Surprise signals in anterior cingulate cortex: neuronal encoding of unsigned reward prediction errors driving adjustment in behavior. *The Journal of neuroscience : the official journal of the Society for Neuroscience*, *31*(11), 4178–4187. https://doi.org/10.1523/JNEUROSCI.4652-10.2011

Hayden, B. Y., Pearson, J. M., & Platt, M. L. (2009). Fictive reward signals in the anterior cingulate cortex. *Science (New York, N.Y.)*, *324*(5929), 948–950. https://doi.org/10.1126/science.1168488

Heilbronner, S. R., & Hayden, B. Y. (2016). *Dorsal anterior cingulate cortex: A bottom-up View*. Annual review of neuroscience. https://www.ncbi.nlm.nih.gov/pmc/articles/PMC5512175/

Hoffstaedter, F., Grefkes, C., Zilles, K., & Eickhoff, S. B. (2013). The "what" and "when" of self-initiated movements. *Cerebral cortex (New York, N.Y. : 1991)*, *23*(3), 520–530.https://doi.org/10.1093/cercor/bhr391

Holt, C. A., & Sullivan, S. P. (2023). Permutation tests for experimental data. *Experimental economics*, 1–38. Advance online publication. https://doi.org/10.1007/s10683-023-09799-6

Hong-Zhi, A., Chen, Z., & Hannan, E.J. (1982). Autocorrelation, Autoregression and Autoregressive Approximation. *Annals of Statistics, 10*, 926-936.

Hoshi, E., Sawamura, H., & Tanji, J. (2005). Neurons in the rostral cingulate motor area monitor multiple phases of visuomotor behavior with modest parametric selectivity. *Journal of neurophysiology*, *94*(1), 640–656. https://doi.org/10.1152/jn.01201.2004

Isomura, Y., Ito, Y., Akazawa, T., Nambu, A., & Takada, M. (2003). Neural coding of "attention for action" and "response selection" in primate anterior cingulate cortex. *The Journal of neuroscience: the official journal of the Society for Neuroscience*, *23*(22), 8002–8012. https://doi.org/10.1523/JNEUROSCI.23-220 8002.2003

Ito, S., Stuphorn, V., Brown, J. W., & Schall, J. D. (2003). Performance monitoring by the anterior cingulate cortex during saccade countermanding. *Science (New York, N.Y.)*, *302*(5642), 120–122. https://doi.org/10.1126/science.1087847

Jenkinson, N., Kühn, A. A., & Brown, P. (2013). Gamma oscillations in the human basal ganglia. *Experimental Neurology*, *245*, 72–76. https://doi.org/10.1016/j.expneurol.2012.07.005

Junod, B., & Wietlisbach, V. (1979). La standardisation, outil d'analyse de données transversales en épidémiologie [Standardization, a tool for the analysis of transversal data in epidemiology]. *Sozial- und Praventivmedizin*, *24*(4), 261. https://doi.org/10.1007/BF02081332

Kennerley, S. W., & Wallis, J. D. (2009). Encoding of reward and space during a working memory task in the orbitofrontal cortex and anterior cingulate sulcus. *Journal of neurophysiology*, *102*(6), 3352–3364. https://doi.org/10.1152/jn.00273.2009

Kennerley, S. W., Behrens, T. E., & Wallis, J. D. (2011). Double dissociation of value computations in orbitofrontal and anterior cingulate neurons. *Nature neuroscience*, *14*(12), 1581–1589. https://doi.org/10.1038/nn.2961

Kennerley, S. W., Walton, M. E., Behrens, T. E., Buckley, M. J., & Rushworth, M. F. (2006). Optimal decision making and the anterior cingulate cortex. *Nature neuroscience*, *9*(7), 940–947. https://doi.org/10.1038/nn1724

Keogh, C., Deli, A., Zand, A. P. D., Zorman, M. J., Boccard-Binet, S. G., Parrott, M., Sigalas, C., Weiss, A. R., Stein, J. F., FitzGerald, J. J., Aziz, T. Z., Green, A. L., & Gillies, M. J. (2022). Spatial and Temporal Distribution of Information Processing in the Human Dorsal Anterior Cingulate Cortex. *Frontiers in human neuroscience*, *16*, 780047.https://doi.org/10.3389/fnhum.2022.780047

Kim, T., Hamade, K. C., Todorov, D., Barnett, W. H., Capps, R. A., Latash, E. M., Markin, S. N., Rybak, I. A., & Molkov, Y. I. (2017). Reward Based Motor Adaptation Mediated by Basal Ganglia. *Frontiers in computational neuroscience*, *11*, 19. https://doi.org/10.3389/fncom.2017.00019

Lanciego, J. L., Luquin, N., & Obeso, J. A. (2012). Functional neuroanatomy of the basal ganglia. *Cold Spring Harbor perspectives in medicine*, *2*(12), a009621. https://doi.org/10.1101/cshperspect.a009621

Lavin, C., Melis, C., Mikulan, E., Gelormini, C., Huepe, D., & Ibañez, A. (2013). The anterior cingulate cortex: an integrative hub for human socially-driven interactions. *Frontiers in neuroscience*, *7*, 64. https://doi.org/10.3389/fnins.2013.00064

Lempka, S. F., & McIntyre, C. C. (2013). Theoretical analysis of the local field potential in deep brain stimulation applications. *PLoS ONE*, *8*(3). https://doi.org/10.1371/journal.pone.0059839

Leske, S., & Dalal, S. S. (2019). Reducing power line noise in EEG and MEG data via spectrum interpolation. *NeuroImage*, *189*, 763–776. https://doi.org/10.1016/j.neuroimage.2019.01.026

Luk, C. H., & Wallis, J. D. (2009). Dynamic encoding of responses and outcomes by neurons in medial prefrontal cortex. *The Journal of neuroscience : the official journal of the Society for Neuroscience*, *29*(23), 7526–7539. https://doi.org/10.1523/JNEUROSCI.0386-09.2009

Makeig, S., Debener, S., Onton, J., & Delorme, A. (2004). Mining event-related brain dynamics. *Trends in cognitive sciences*, *8*(5), 204–210. https://doi.org/10.1016/j.tics.2004.03.008

Mao, Z., Ling, Z., Pan, L., Xu, X., Cui, Z., Liang, S., & Yu, X. (2019). Comparison of Efficacy of Deep Brain Stimulation of Different Targets in Parkinson's Disease: A Network Meta-Analysis. *Frontiers in aging neuroscience*, *11*, 23. https://doi.org/10.3389/fnagi.2019.00023

Matsumoto, K., Suzuki, W., & Tanaka, K. (2003). Neuronal correlates of goal-based motor selection in the prefrontal cortex. *Science (New York, N.Y.)*, *301*(5630), 229–232. https://doi.org/10.1126/science.1084204

Matsumoto, M., Matsumoto, K., Abe, H., & Tanaka, K. (2007). Medial prefrontal cell activity signaling prediction errors of action values. *Nature neuroscience*, *10*(5), 647–656. https://doi.org/10.1038/nn1890

Matthews, S. C., Paulus, M. P., Simmons , A. N., Nelesen, R. A., & Dimsdale, J. E. (2004). *Functional subdivisions within anterior cingulate cortex and their relationship to autonomic nervous system function*. Science Direct . https://www.sciencedirect.com/science/article/pii/S1053811904001491?via=ihub

McIntyre, C. C., Savasta, M., Walter, B. L., & Vitek, J. L. (2004). How does deep brain stimulation work? Present understanding and future questions. *Journal of clinical neurophysiology : official publication of the American Electroencephalographic Society*, *21*(1), 40–50. https://doi.org/10.1097/00004691-200401000-00006

Mishchenko, Y. (Gene). (2021). *Bootstrapping vs permutation testing*. Medium. https://towardsdatascience.com/bootstrapping-vs-permutation-testing-a30237795970

Morecraft, R. J., & Van Hoesen, G. W. (1998). Convergence of limbic input to the cingulate motor cortex in the rhesus monkey. *Brain research bulletin*, *45*(2), 209–232. https://doi.org/10.1016/s0361-9230(97)00344-4

Mulcahy, G., Atwood, B., & Kuznetsov, A. (2020). Basal ganglia role in learning rewarded actions and executing previously learned choices: Healthy and diseased states. *PloS one*, *15*(2), e0228081.https://doi.org/10.1371/journal.pone.0228081

Nakamura, K., Roesch, M. R., & Olson, C. R. (2005). Neuronal activity in macaque SEF and ACC during performance of tasks involving conflict. *Journal of neurophysiology*, *93*(2), 884–908. https://doi.org/10.1152/jn.00305.2004

Palumbo, R., Di Domenico, A., Fairfield, B., & Mammarella, N. (2021). When twice is better than once: increased liking of repeated items influences memory in younger and older adults. *BMC Psychology*, *9*(1). https://doi.org/10.1186/s40359-021-00531-8

Paus T. (2001). Primate anterior cingulate cortex: where motor control, drive and cognition interface. *Nature reviews. Neuroscience*, *2*(6), 417–424. https://doi.org/10.1038/35077500

Perlmutter, J. S., & Mink, J. W. (2006). Deep brain stimulation. *Annual review of neuroscience*, *29*, 229–257. https://doi.org/10.1146/annurev.neuro.29.051605.112824

Prerau Lab. (2021). *Introduction to Spectral Analysis for sleep Research: From fourier to Multitaper: Dr. Michael Prerau* [Video]. YouTube. https://www.youtube.com/watch?v=vJ6a0f0zR1E

Procyk, E., Tanaka, Y. L., & Joseph, J. P. (2000). Anterior cingulate activity during routine and non routine sequential behaviors in macaques. *Nature neuroscience*, *3*(5), 502–508. https://doi.org/10.1038/74880

Procyk, E., Wilson, C. R., Stoll, F. M., Faraut, M. C., Petrides, M., & Amiez, C. (2016). Midcingulate Motor Map and Feedback Detection: Converging Data from Humans and Monkeys. *Cerebral cortex (New York, N.Y. : 1991)*, *26*(2), 467–476.https://doi.org/10.1093/cercor/bhu213

Quilodran, R., Rothé, M., & Procyk, E. (2008). Behavioral shifts and action valuation in the anterior cingulate cortex. *Neuron*, *57*(2), 314–325. https://doi.org/10.1016/j.neuron.2007.11.031

Rescorla, RA & Wagner, Allan. (1972). A theory of Pavlovian conditioning: Variations in the effectiveness of reinforcement and nonreinforcement. In A.H. Black & W.F Prokasy, Eds., Classical Conditioning II, pp.64-69. Appleton-Century-Crofts

Rouam, S. (1970). *False discovery rate (FDR)*. SpringerLink. https://link.springer.com/referenceworkentry/10.1007/978-1-4419-9863-7_223#:~:text=The%20false%20discovery%20rate%20(FDR,events%20that%20falsely%20appear%20significant

Rouhani, N., & Niv, Y. (2021). Signed and unsigned reward prediction errors dynamically enhance learning and memory. *eLife*, *10*, e61077. https://doi.org/10.7554/eLife.61077

Rushworth, M. F., Hadland, K. A., Gaffan, D., & Passingham, R. E. (2003). The effect of cingulate cortex lesions on task switching and working memory. *Journal of cognitive neuroscience*, *15*(3), 338–353. https://doi.org/10.1162/089892903321593072

Seo, H., & Lee, D. (2007). Temporal filtering of reward signals in the dorsal anterior cingulate cortex during a mixed-strategy game. *The Journal of neuroscience : the official journal of the Society for Neuroscience*, *27*(31), 8366–8377. https://doi.org/10.1523/JNEUROSCI.2369-07.2007

Shima, K., & Tanji, J. (1998). Role for cingulate motor area cells in voluntary movement selection based on reward. *Science (New York, N.Y.)*, *282*(5392), 1335–1338. https://doi.org/10.1126/science.282.5392.1335

Shima, K., Aya, K., Mushiake, H., Inase, M., Aizawa, H., & Tanji, J. (1991). Two movement-related foci in the primate cingulate cortex observed in signal-triggered and self-paced forelimb movements. *Journal of neurophysiology*, *65*(2), 188–202. https://doi.org/10.1152/jn.1991.65.2.188

Sironi V. A. (2011). Origin and evolution of deep brain stimulation. *Frontiers in integrative neuroscience*, *5*, 42. https://doi.org/10.3389/fnint.2011.00042

Smith, N. J., & Kutas, M. (2014). Regression-based estimation of ERP waveforms: I. The rERP framework. *Psychophysiology*, *52*(2), 157–168. https://doi.org/10.1111/psyp.12317

Stephanie. (2023). *False discovery rate: Simple definition, adjusting for FDR*. Statistics How To. https://www.statisticshowto.com/false-discovery-rate/

Steve Brunton. (2020). *The Fast Fourier Transform (FFT)* [Video]. YouTube. https://www.youtube.com/watch?v=E8HeD-MUrjY

Stevens, F. L., Hurley, R. A., & Taber, K. H. (2011). Anterior cingulate cortex: unique role in cognition and emotion. *The Journal of neuropsychiatry and clinical neurosciences*, *23*(2), 121–125. https://doi.org/10.1176/jnp.23.2.jnp121

Strait, C. E., Sleezer, B. J., Blanchard, T. C., Azab, H., Castagno, M. D., & Hayden, B. Y. (2016). Neuronal selectivity for spatial positions of offers and choices in five reward regions. *Journal of neurophysiology*, *115*(3), 1098–1111. https://doi.org/10.1152/jn.00325.2015

Sur, S., & Sinha, V. K. (2009). Event-related potential: An overview. *Industrial psychiatry journal*, *18*(1), 70–73. https://doi.org/10.4103/0972-6748.57865

Talebi, S. (2022). Fourier vs. Wavelet Transform: What's the Difference? *Built In*. https://builtin.com/data-science/wavelet-transform#

The MathWorks Inc. (2022). MATLAB version: 9.13.0 (R2022b), Natick, Massachusetts: The MathWorks Inc. https://www.mathworks.com

Touroutoglou, A., Andreano, J., Dickerson, B. C., & Barrett, L. F. (2020). The tenacious brain: How the anterior mid-cingulate contributes to achieving goals. *Cortex*, *123*, 12–29. https://doi.org/10.1016/j.cortex.2019.09.011

Turing. (2022). Guide to Autoregressive Models. *www.turing.com*. https://www.turing.com/kb/guide-to-autoregressive-models#

Weiss, A. R., Gillies, M. J., Philiastides, M. G., Apps, M. A., Whittington, M. A. FitzGerald, J. J., Boccard, S. G., Aziz, T. Z., & Green, A. L. (2018). Dorsal Anterior Cingulate Cortices Differentially Lateralize Prediction Errors and Outcome Valence in a Decision-Making Task. *Frontiers in human neuroscience*, *12*, 203. https://doi.org/10.3389/fnhum.2018.00203

Williams, Z. M., Bush, G., Rauch, S. L., Cosgrove, G. R., & Eskandar, E. N. (2004). Human anterior cingulate neurons and the integration of monetary reward with motor responses. *Nature neuroscience*, *7*(12), 1370–1375.https://doi.org/10.1038/nn1354

Womelsdorf, T., Johnston, K., Vinck, M., & Everling, S. (2010). Theta-activity inanterior cingulate cortex predicts task rules and their adjustments following errors. *Proceedings of the National Academy of Sciences of theUnited States of America*, *107*(11), 5248–5253. https://doi.org/10.1073/pnas.0906194107

Woodman G. F. (2010). A brief introduction to the use of event-related potentials in studies of perception and attention. *Attention, perception & psychophysics*, *72*(8), 2031–2046. https://doi.org/10.3758/APP.72.8.2031

Zhang, Z., & Koike, Y. (2022). Clustered event related spectral perturbation (ERSP) feature in right hand motor imagery classification. *Frontiers in neuroscience*, *16*, 867480. https://doi.org/10.3389/fnins.2022.8674802